Wireless Pers Commun
DOI 10.1007/s11277-007-9281-4

Spatial precoder design for space–time coded MIMO systems: based on fixed parameters of MIMO channels

Tharaka A. Lamahewa · Rodney A. Kennedy · Thushara D. Abhayapala · Van K. Nguyen

Received: 30 April 2006 / Accepted: 15 February 2007

Abstract In realistic channel environments the performance of space–time coded multiple-input multiple output (MIMO) systems is significantly reduced due to non-ideal antenna placement and non-isotropic scattering. In this paper, by exploiting the spatial dimension of a MIMO channel we introduce the novel idea of linear spatial precoding (or power-loading) based on fixed and known parameters of MIMO channels to ameliorate the effects of non-ideal antenna placement on the performance of coherent (channel is known at the receiver) and non-coherent (channel is un-known at the receiver) space–time codes. Antenna spacing and antenna placement (geometry) are considered as fixed parameters of MIMO channels, which are readily known at the transmitter. With this design, the precoder is fixed for fixed antenna placement and the transmitter does not require any feedback of channel state information (partial or full) from the receiver. We also derive precoding schemes to exploit non-isotropic scattering distribution parameters of the scattering channel to improve the performance of space–time codes applied on MIMO systems. However, these schemes require the receiver to estimate the non-isotropic parameters and feed them back to the transmitter. Closed form solutions for precoding schemes are presented for systems with up to three receive antennas. A generalized method is proposed for more than three receive antennas.

Keywords Space–time coding · Channel modelling · Linear precoder design · MIMO systems · Non-isotropic scattering · Spatial correlation

1 Introduction

Multiple input multiple output (MIMO) communication systems that use multi-antenna arrays simultaneously during transmission and reception have generated significant interest in recent years. Under the assumption of fading channel coefficients between different antenna elements are statistically independent and fully known at the receiver (coherent detection), theoretical work of [1,2] revealed that the channel capacity of multiple-antenna array communication systems scales linearly with the smaller of the number of transmit and receive antennas. Motivated by these works [3–5], have proposed several modulation and coding schemes, namely space–time trellis codes and space–time block codes, to exploit the potential increase in capacity, and diversity gains using multi antenna arrays with coherent detection.

In practise, insufficient antenna spacing, non-ideal antenna placement and non-isotropic scattering environments cause individual antennas in an antenna array

T. A. Lamahewa (✉) · R. A. Kennedy · T. D. Abhayapala
Department of Information Engineering, Research School of Information Sciences and Engineering, The Australian National University, Canberra, ACT 0200, Australia.
e-mail: tharaka.lamahewa@anu.edu.au

V. K. Nguyen
School of Engineering and Technology, Deakin University, Geelong, VIC 3217, Australia

to be correlated, leading to loss of performance from multi-antenna wireless communication systems. This has motivated the design of linear precoders (or power loading schemes) for multi-antenna wireless communication systems by exploiting the statistical information of the MIMO channels [6–12]. In these designs, the receiver either feeds back the full channel state information (CSI) or the partial CSI (e.g., correlation coefficients of the channel) to the transmitter via a low-rate feedback channel.

In [6], a joint transmit and receive optimization scheme for MIMO spatial multiplexing systems in narrowband wireless channels is proposed by minimizing the mean square error of received signals. This scheme requires the receiver to feedback the full CSI to the transmitter. In [7], by minimizing the channel estimation error variance a general criteria to design optimal transmitter precoders is proposed for stationary random fading channels. The optimal design requires the knowledge of the channel's correlation matrix. In [8–10], linear precoding schemes are developed based on channel correlation matrix for *coherent* space–time block coded wireless communication systems. In [8], the precoder is designed by minimizing the bit error rate and symbol error rate expressions of space–time block coded (STBC) MISO systems. In [9,10], the pairwise error probability (PEO) upper bound of STBC has been used as the cost function. In [9], the optimum precoder is derived in closed form for a MISO system and presented a numerical solution for MIMO systems assuming a Kronecker type scattering channel. In [10], the precoder is derived for a non-Kronecker type scattering channel. However, this design assumed a block diagonal structure for the correlation matrix of the MIMO channel. Linear precoding schemes for *non-coherent differential* space–time block coded systems are developed in [11,12] based on channel correlation feedback. In [11], the Chernoff bound of approximate symbol error rate of differential STBC is minimized to obtain the precoder for a MISO system. Assuming an uncorrelated receiver antenna array and arbitrary correlation at the transmitter antenna array [12], has derived a linear precoding scheme similar to that of [11].

In order to be cost effective and optimal, linear precoding schemes proposed in the literature assumed that the channel remains stationary (channel statistics are invariant) for a large number of symbol periods and the transmitter is capable of acquiring robust channel state information. However, when the channel is non-stationary or it is stationary for a small number of symbol periods, the receiver will have to feedback the channel information to the transmitter frequently. As a result, the system becomes costly and the optimum precoder design, based on the previously possessed information, becomes outdated quickly. In some circumstances feeding back channel information is not possible. These facts have motivated us to design a precoding scheme based on fixed and known parameters of the underlying MIMO channel.

In this paper, we introduce the novel use of linear spatial precoding based on fixed and known parameters of MIMO channels to improve the performance of both coherent and non-coherent space–time coded MIMO systems. Spatial precoding schemes are designed based on previously unutilized fixed and known parameters of MIMO channels, namely the antenna spacing and antenna placement (geometry) details. These precoding schemes exploit the antenna placement information at both ends of the MIMO channel to ameliorate the effect of non-ideal antenna placement on the performance of space–time coded systems. Both precoding schemes are fixed for fixed antenna placement and the transmitter does not require any form of feedback of channel state information (partial or full) from the receiver. Since the designs are fixed for given transmitter and receiver antenna configurations, these spatial precoders can be used in non-stationary channels as well as stationary channels. In addition, we develop precoding schemes to exploit the non-isotropic parameters to improve the performance of space–time coded systems applied on MIMO channels in non-isotropic scattering environments. Unlike in the first fixed scheme, this scheme requires the receiver to estimate the non-isotropic parameters of the scattering channel (mean angle of arrival/departure, angular spread) and feed them back to the transmitter.

In this paper, we also derive upper bounds for the PEP of coherent space–time codes and differential space–time codes for spatially correlated MIMO fading channels. To the authors knowledge, the PEP upper bound of differential space–time codes is a new bound. Utilizing the MIMO channel decomposition given in [13], antenna configuration details and scattering environment parameters (angular spreads and mean angle of arrival and departure) are incorporated in to these PEP upper bounds. The optimum precoders are derived by minimizing these PEP expressions subject to a transmit power constraint. Closed form solutions for both precoding schemes are presented for systems with up to three receive antennas and a generalized method is proposed for more than three receive antennas.

An outline of the paper is as follows. Section 2 reviews the spatial channel model used in our design. In Section 3, the precoded coherent STBC and differential STBC systems are described along with detection rules at the receiver. Sections 4 and 5 present the optimization problem and the optimal precoder solution for coherent STBC and differential STBC, respectively. Sections 6 and 7 present performance results obtained with proposed precoding schemes for various spatial scenarios using the spatial channel model in [13] as the underlying MIMO channel. Section 8 presents the simulation results of our proposed precoding schemes applied on other statistical channel models found in the literature. Section 9 presents some concluding remarks.

Notations Throughout the paper, the following notations will be used: bold lower (upper) letters denote vectors (matrices). $[\cdot]^T$, $[\cdot]^*$, and $[\cdot]^\dagger$ denote the transpose, complex conjugate, and conjugate transpose operations, respectively. The symbol $\otimes$ denotes the Matrix Kronecker product. The notation $E\{\cdot\}$ denotes the mathematical expectation, $\text{vec}\{\mathbf{A}\}$ denotes the vectorization operator which stacks the columns of $\mathbf{A}$, $\text{tr}\{\cdot\}$ denotes the matrix trace, $\lceil . \rceil$ denotes the ceiling operator, and $\mathbb{S}^1$ denotes the unit circle. The matrix $\mathbf{I}_n$ is the $n \times n$ identity matrix.

2 Spatial channel model

First, we review the spatial channel model proposed in [13]. Consider a MIMO system consisting of n_T transmit antennas located at positions $\mathbf{u}_t$, $t = 1, 2, \ldots, n_\text{T}$ relative to the transmitter array origin, and n_R receive antennas located at positions $\mathbf{v}_r$, $r = 1, 2, \ldots, n_\text{R}$ relative to the receiver array origin. We assume that scatterers are distributed in the far field from the transmit and receive antennas, and regions containing the transmit and receive antennas are distinct.

Here we consider the situation where the multi-path is restricted to the azimuth plane only (2D scattering environment), having no field components arriving at significant elevations. In this case, by taking into account physical aspects of scattering, the MIMO channel matrix $\mathbf{H}$ can be decomposed into deterministic and random parts as [13]

$$\mathbf{H} = \mathbf{J}_\text{R}\mathbf{H}_\text{S}\mathbf{J}_\text{T}^\dagger, \tag{1}$$

where $\mathbf{J}_\text{R}$ is the $n_\text{R} \times (2N_\text{R}+1)$ deterministic receiver configuration matrix,

$$\mathbf{J}_\text{R} = \begin{bmatrix} \mathcal{J}_{-N_\text{R}}(\mathbf{v}_1) & \cdots & \mathcal{J}_{N_\text{R}}(\mathbf{v}_1) \\ \mathcal{J}_{-N_\text{R}}(\mathbf{v}_2) & \cdots & \mathcal{J}_{N_\text{R}}(\mathbf{v}_2) \\ \vdots & \ddots & \vdots \\ \mathcal{J}_{-N_\text{R}}(\mathbf{v}_{n_\text{R}}) & \cdots & \mathcal{J}_{N_\text{R}}(\mathbf{v}_{n_\text{R}}) \end{bmatrix}$$

and $\mathbf{J}_\text{T}$ is the $n_\text{T} \times (2N_\text{T}+1)$ deterministic transmitter configuration matrix,

$$\mathbf{J}_\text{T} = \begin{bmatrix} \mathcal{J}_{-N_\text{T}}(\mathbf{u}_1) & \cdots & \mathcal{J}_{N_\text{T}}(\mathbf{u}_1) \\ \mathcal{J}_{-N_\text{T}}(\mathbf{u}_2) & \cdots & \mathcal{J}_{N_\text{T}}(\mathbf{u}_2) \\ \vdots & \ddots & \vdots \\ \mathcal{J}_{-N_\text{T}}(\mathbf{u}_{n_\text{T}}) & \cdots & \mathcal{J}_{N_\text{T}}(\mathbf{u}_{n_\text{T}}) \end{bmatrix}$$

with

$$\mathcal{J}_n(\mathbf{w}) \triangleq J_n(\kappa_0\|\mathbf{w}\|)e^{\imath n(\phi_w - \pi/2)}$$

defined as the spatial-to-mode function which maps the antenna location $\mathbf{w}$ to the nth mode of the region, where $J_n(\cdot)$ is the Bessel function of integer order n, $\mathbf{w} \equiv (\|\mathbf{w}\|, \phi_w)$ in polar coordinates is the antenna location relative to the origin of the aperture, $\kappa_0 = 2\pi/\lambda$ is the wave number with λ being the wave length and $\imath = \sqrt{-1}$. $2N_\text{T}+1$ and $2N_\text{R}+1$ are the number of effective[1] communication modes at the transmit and receive regions, respectively. Note, N_T and N_R are defined by the size of the regions containing all the transmit and receive antennas, respectively [14]. In our case,

$$N_\text{T} = \left\lceil \frac{\pi e r_\text{T}}{\lambda} \right\rceil \quad \text{and}$$
$$N_\text{R} = \left\lceil \frac{\pi e r_\text{R}}{\lambda} \right\rceil,$$

where $e \approx 2.7183$.

Finally, $\mathbf{H}_\text{S}$ is the $(2N_\text{R}+1) \times (2N_\text{T}+1)$ random complex scattering channel matrix with (ℓ, m)th element given by

$$\{\mathbf{H}_\text{S}\}_{\ell,m} = \iint_{\mathbb{S}^1\times\mathbb{S}^1} g(\phi,\varphi)e^{\imath(m-N_\text{T}-1)\phi}e^{-\imath(\ell-N_\text{R}-1)\varphi}\, \mathrm{d}\phi\mathrm{d}\varphi \tag{2}$$

representing the complex scattering gain between the $(m - N_\text{T} - 1)$th mode of the scatter-free transmitter region and $(\ell - N_\text{R} - 1)$th mode of the scatter-free receiver region, where $g(\phi, \varphi)$ is the effective random

[1] Although there are infinite number of modes excited by an antenna array, there are only finite number of modes $(2N + 1)$ which have sufficient power to carry information.

complex scattering gain function for signals with angle-of-departure ϕ from the scatter-free transmitter region and angle-of-arrival φ at the scatter-free receiver region.

The channel matrix decomposition (1) separates the channel into three distinct regions of interest: the scatter-free region around the transmitter antenna array, the scatter-free region around the receiver antenna array, and the complex random scattering environment which is the complement of the union of two antenna array regions. Consequently, the MIMO channel is decomposed into deterministic and random matrices, where deterministic portions $\mathbf{J}_\mathrm{T}$ and $\mathbf{J}_\mathrm{R}$ represent the physical configuration of the transmitter and the receiver antenna arrays, respectively, and the random portion represents the complex scattering environment between the transmitter and the receiver antenna regions. The reader is referred to [13] for more information regarding this spatial channel model. Note that the precoder design is based on this channel model, but the performance does not depend on this model (see Sect. 8). That is, our design and simulations provide an independent confirmation of the validity and usefulness of this channel model.

Here we assume that the azimuth power distribution $\mathcal{P}(\varphi)$ at the receiver region is independent of the azimuth power distribution $\mathcal{P}(\phi)$ at the transmitter region, i.e.,

$$E\left\{|g(\phi,\varphi)|^2\right\} = G(\phi,\varphi) = \mathcal{P}(\phi)\mathcal{P}(\varphi)$$

with $\int\int G(\phi,\varphi)\mathrm{d}\varphi\mathrm{d}\phi = 1$, then the correlation matrix of the channel (1) can be written as [15]

$$\mathbf{R}_\mathrm{H} = E\left\{\mathbf{h}^\dagger\mathbf{h}\right\} = \left(\mathbf{J}_\mathrm{R}^*\mathbf{F}_\mathrm{R}\mathbf{J}_\mathrm{R}^T\right) \otimes \left(\mathbf{J}_\mathrm{T}\mathbf{F}_\mathrm{T}\mathbf{J}_\mathrm{T}^\dagger\right), \tag{3}$$

where $\mathbf{h} = (\mathrm{vec}\{\mathbf{H}^T\})^T$, $\mathbf{F}_\mathrm{R}$, and $\mathbf{F}_\mathrm{T}$ are modal[2] correlation matrices at the receiver and the transmitter, respectively. Note that (3) is mathematically identical to the so called Kronecker model. The (ℓ,ℓ')th element of $\mathbf{F}_\mathrm{R}$ and the (m,m')th element of $\mathbf{F}_\mathrm{T}$ are given by

$$\{\mathbf{F}_\mathrm{R}\}_{\ell,\ell'} = \int_{\mathbb{S}^1}\mathcal{P}(\varphi)e^{-i(\ell-\ell')\varphi}\mathrm{d}\varphi,$$
$$\{\mathbf{F}_\mathrm{T}\}_{m,m'} = \int_{\mathbb{S}^1}\mathcal{P}(\phi)e^{i(m-m')\phi}\mathrm{d}\phi.$$

Usually, APD is characterized by the mean angle of arrival/departure and angular spread. Note that we have "rich" scattering when $\mathbf{F}_\mathrm{R} = \mathbf{I}$ and $\mathbf{F}_\mathrm{T} = \mathbf{I}$.

[2] The set of modes form a basis of functions for representing a multi-path wave field [13].

3 System model

At time instance k, the space time encoder at the transmitter takes a set of modulated symbols[3] $\mathbf{C}(k) = \{c_1(k), c_2(k), \ldots, c_K(k)\}$ and maps them onto an $n_\mathrm{T}\times L$ code word matrix $\mathbf{S}_{\ell(k)} \in \mathcal{V}$ of unitary space–time modulated constellation matrices set $\mathcal{V} \equiv \{\mathbf{S}_\ell|\mathbf{S}_\ell\mathbf{S}_\ell^\dagger = \mathbf{I}_{n_\mathrm{T}}, \ell = 1,2,\ldots,T\}$, where L is the code length, $T = q^K$ and q is the size of the constellation from which $c_n(k)$, $n = 1,\ldots,K$ are drawn with $\ell(k) = 1,2,\ldots,T$.

In this paper, we mainly focus on the space–time modulated constellations with the property

$$(\mathbf{S}_i - \mathbf{S}_j)(\mathbf{S}_i - \mathbf{S}_j)^\dagger = \beta_{i,j}\mathbf{I}_{n_\mathrm{T}}, \quad \forall\, i \neq j, \tag{4}$$

where $\beta_{i,j}$ is a scalar and $\mathbf{S}_i, \mathbf{S}_j \in \mathcal{V}$. Space-time orthogonal designs in [5] and some cyclic and dicyclic space–time modulated constellations in [16] are some examples which satisfy property (4) above.

3.1 Coherent space–time block codes

Let $\mathbf{s}_n$ be the nth column of $\mathbf{S}_i = [\mathbf{s}_1,\mathbf{s}_2,\ldots,\mathbf{s}_L] \in \mathcal{V}$. At the transmitter, each code vector $\mathbf{s}_n$ is multiplied by a $n_\mathrm{T}\times n_\mathrm{T}$ fixed linear precoder matrix $\mathbf{F}_\mathrm{c}$ before transmitting out from n_T transmit antennas. Assuming quasi-static fading, the signals received at n_R receive antennas during L symbol periods can be expressed in matrix form as

$$\mathbf{Y}(k) = \sqrt{E_\mathrm{s}}\mathbf{H}\mathbf{F}_\mathrm{c}\mathbf{S}_{\ell(k)} + \mathbf{N}(k),$$

where E_s is the average transmitted signal energy per symbol period, $\mathbf{N}(k)$ is the $n_\mathrm{R}\times L$ white Gaussian noise matrix in which elements are zero-mean independent Gaussian distributed random variables with variance $\sigma_n^2/2$ per dimension and $\mathbf{H}$ is the $n_\mathrm{R}\times n_\mathrm{T}$ channel matrix. In this work, we use the channel decomposition (1) to represent the underlying MIMO channel and the elements of scattering channel matrix $\mathbf{H}_S$ are modeled as zero-mean complex Gaussian random variables (Rayleigh fading).

For coherent STBC, we assume that the receiver has perfect CSI and transmitter has partial CSI. At the receiver, the transmitted codeword is detected by applying the maximum likelihood (ML) detection rule:

$$\begin{aligned}\widehat{\mathbf{S}}_{\ell(k)} &= \arg\min_{\mathbf{S}_{\ell(k)}\in\mathcal{V}} \parallel \mathbf{y}(k) - \sqrt{E_\mathrm{s}}\,\widetilde{\mathbf{h}}\mathcal{S}_{\ell(k)} \parallel^2,\\ &= \arg\max_{\mathbf{S}_{\ell(k)}\in\mathcal{V}} \mathrm{Re}\{\widetilde{\mathbf{h}}\,\mathcal{S}_{\ell(k)}\,\mathbf{y}^\dagger(k)\},\end{aligned} \tag{5}$$

[3] Modulated symbols are normalized such that $|c_n(k)| = 1/\sqrt{K}$.

where $\mathbf{y}(k) = (\mathrm{vec}\{\mathbf{Y}^T(k)\})^T$, $\mathcal{S}_{\ell(k)} = \mathbf{I}_{n_\mathrm{R}} \otimes \mathbf{S}_{\ell(k)}$, and $\widetilde{\mathbf{h}} = (\mathrm{vec}\{\widetilde{\mathbf{H}}^T\})^T$ with $\widetilde{\mathbf{H}} = \mathbf{H}\mathbf{F}_\mathrm{c}$.

3.2 Differential space–time block codes

In this scheme, codeword matrix $\mathbf{S}_{\ell(k)}$ is differentially encoded according to the rule

$$\mathbf{X}(k) = \mathbf{X}(k-1)\mathbf{S}_{\ell(k)} \quad \text{for } k = 1, 2, \ldots$$

with $\mathbf{X}(0) = \mathbf{I}_{n_\mathrm{T}}$. Then, each encoded $\mathbf{X}(k)$ is multiplied by a $n_\mathrm{T} \times n_\mathrm{T}$ fixed linear precoder matrix $\mathbf{F}_\mathrm{d}$ before transmitting out from n_T transmit antennas. Similar to [16,19], we assume that code length $L = n_\mathrm{T}$. With this assumption, each code word matrix $\mathbf{S}_i$ in $\mathcal{V}$ will satisfy the unitary property $\mathbf{S}_{\ell(k)}\mathbf{S}^\dagger_{\ell(k)} = \mathbf{I}_{n_\mathrm{T}}$ and $\mathbf{S}^\dagger_{\ell(k)}\mathbf{S}_{\ell(k)} = \mathbf{I}_{n_\mathrm{T}}$ for $\ell(k) = 1, 2, \ldots, T$. As a result, $\mathbf{X}(k)$ will also satisfy the unitary property $\mathbf{X}(k)\mathbf{X}^\dagger(k) = \mathbf{I}$ and $\mathbf{X}^\dagger(k)\mathbf{X}(k) = \mathbf{I}$ for $k = 0, 1, 2, \ldots$.

Assuming quasi-static fading, the signals received at n_R receive antennas during n_T symbol periods can be expressed in matrix form as

$$\mathbf{Y}(k) = \sqrt{E_\mathrm{s}}\mathbf{H}\mathbf{F}_\mathrm{d}\mathbf{X}(k) + \mathbf{N}(k),$$

where $\mathbf{N}(k)$ is the $n_\mathrm{R} \times n_\mathrm{T}$ white Gaussian noise matrix in which elements are zero-mean independent Gaussian distributed random variables with variance $\sigma_n^2/2$ per complex dimension and $\mathbf{H}$ is the $n_\mathrm{R} \times n_\mathrm{T}$ channel matrix, which is modeled using (1).

Assume that the scattering channel matrix $\mathbf{H}_\mathrm{S}$ remains constant during the reception of two consecutive received signal blocks $\mathbf{Y}(k-1)$ and $\mathbf{Y}(k)$, which can be expressed in vector (row) form as

$$\begin{aligned} \mathbf{y}(k-1) &= \sqrt{E_\mathrm{s}}\mathbf{h}\mathcal{X}_\mathrm{d}(k-1) + \mathbf{n}(k-1), \\ \mathbf{y}(k) &= \sqrt{E_\mathrm{s}}\mathbf{h}\mathcal{X}_\mathrm{d}(k) + \mathbf{n}(k), \\ &= \mathbf{y}(k-1)\mathcal{S}_{\ell(k)} + \mathbf{w}(k), \end{aligned} \tag{6}$$

where $\mathbf{y}(k) = (\mathrm{vec}\{\mathbf{Y}(k)^T\})^T$, $\mathcal{X}_\mathrm{d}(k) = \mathbf{I}_{n_\mathrm{R}} \otimes (\mathbf{F}_\mathrm{d}\mathbf{X}(k))$, $\mathbf{h} = (\mathrm{vec}\{\mathbf{H}^T\})^T$, $\mathbf{n}(k) = (\mathrm{vec}\{\mathbf{N}(k)^T\})^T$, $\mathcal{S}_{\ell(k)} = \mathbf{I}_{n_\mathrm{R}} \otimes \mathbf{S}_{\ell(k)}$, and $\mathbf{w}(k) = \mathbf{n}(k) - \mathbf{n}(k-1)\mathcal{S}_{\ell(k)}$.

For differential STBC, we assume that the receiver has no CSI whilst the transmitter has partial CSI. From (6), the transmitted codeword matrix is detected differentially using the ML detection rule:

$$\begin{aligned} \widehat{\mathbf{S}}_{\ell(k)} &= \arg\min_{\mathbf{S}_{\ell(k)} \in \mathcal{V}} \| \mathbf{y}(k) - \mathbf{y}(k-1)\mathcal{S}_{\ell(k)} \|^2, \\ &= \arg\max_{\mathbf{S}_{\ell(k)} \in \mathcal{V}} \mathrm{Re}\{\mathbf{y}(k-1)\mathcal{S}_{\ell(k)}\mathbf{y}(k)^\dagger\}. \end{aligned}$$

4 Problem setup: Coherent STBC

Assume that perfect CSI is available at the receiver and also ML detection is employed at the receiver. Suppose codeword $\mathbf{S}_i \in \mathcal{V}$ is transmitted, but the ML-decoder (5) chooses codeword $\mathbf{S}_j \in \mathcal{V}$, then as shown in the Appendix A, the average PEP is upper bounded by

$$\mathrm{P}(\mathbf{S}_i \to \mathbf{S}_j) \le \frac{1}{\det\left(\mathbf{I}_{n_\mathrm{T} n_\mathrm{R}} + \frac{\overline{\gamma}}{4}\mathbf{R}_\mathrm{H}[\mathbf{I}_{n_\mathrm{R}} \otimes \mathbf{S}_{\Delta,\mathbf{F}_\mathrm{c}}]\right)}, \tag{7}$$

where $\mathbf{S}_{\Delta,\mathbf{F}_\mathrm{c}} = \mathbf{F}_\mathrm{c}(\mathbf{S}_i - \mathbf{S}_j)(\mathbf{S}_i - \mathbf{S}_j)^\dagger\mathbf{F}_\mathrm{c}^\dagger$, $\overline{\gamma} = E_s/\sigma_n^2$ is the average symbol energy-to-noise ratio (SNR) at each receive antenna and $\mathbf{R}_\mathrm{H}$ is the correlation matrix of the MIMO channel $\mathbf{H}$ given by(3).

By applying the property (4) associated with orthogonal space–time block codes, we can simplify the PEP upper-bound (7) to

$$\mathrm{P}(\mathbf{S}_i \to \mathbf{S}_j) \le \frac{1}{\det\left(\mathbf{I}_{n_\mathrm{T} n_\mathrm{R}} + \frac{\overline{\gamma}\beta_{i,j}}{4}\mathbf{R}_\mathrm{H}\left[\mathbf{I}_{n_\mathrm{R}} \otimes \left(\mathbf{F}_\mathrm{c}\mathbf{F}_\mathrm{c}^\dagger\right)\right]\right)}. \tag{8}$$

In this work, our main objective is to find the optimum precoding scheme which reduces the spatial correlation effects on the performance of coherent STBC. We achieve this by minimizing the average PEP bound (8) subject to the transmit power constraint $\mathrm{tr}\{\mathbf{F}_\mathrm{c}\mathbf{F}_\mathrm{c}^\dagger\} = n_\mathrm{T}$. Here we propose two schemes for the optimal precoder $\mathbf{F}_\mathrm{c}$ by considering two scenarios for the channel correlation matrix $\mathbf{R}_\mathrm{H}$. The two optimization problems can be stated as follows:

Scheme 1 ***Fixed scheme (coherence)****: find the optimum $\mathbf{F}_\mathrm{c}$ that minimizes the average PEP upper bound* (8) *for coherent STBC, subject to the transmit power constraint tr$\{\mathbf{F}_\mathrm{c}\mathbf{F}_\mathrm{c}^\dagger\} = n_\mathrm{T}$, for given transmitter and receiver antenna configurations assuming a rich scattering environment.*

In this case, the channel correlation matrix[4] $\mathbf{R}_\mathrm{H}$ is given by,

$$\mathbf{R}_\mathrm{H} = \left(\mathbf{J}_\mathrm{R}^*\mathbf{J}_\mathrm{R}^T\right) \otimes \left(\mathbf{J}_\mathrm{T}\mathbf{J}_\mathrm{T}^\dagger\right).$$

Since $\mathbf{J}_\mathrm{R}$ and $\mathbf{J}_\mathrm{T}$ are fixed and deterministic for given antenna configurations, the **precoder is fixed**. Therefore, in this scheme, the transmitter does not require any feedback information about the channel to derive the optimum precoder $\mathbf{F}_\mathrm{c}$. This precoding scheme exploits the antenna placement information at both ends

[4] The Kronecker channel assumption can be relaxed in this case.

of the MIMO channel to compensate for any detrimental effects of non-ideal antenna placement on the performance of coherent space time block codes.

Scheme 2 ***Feedback scheme (coherence)****: find the optimum* $\mathbf{F}_\mathrm{c}$ *that minimizes the average PEP upper bound* (8) *for coherent STBC, subject to the transmit power constraint* $tr\{\mathbf{F}_\mathrm{c}\mathbf{F}_\mathrm{c}^\dagger\} = n_\mathrm{T}$*, for given transmitter and receiver antenna configurations assuming the receiver estimates the non-isotropic distribution parameters and feeds them back to the transmitter.*

Note that the optimum precoder $\mathbf{F}_\mathrm{c}$ in scheme-2 exploits the non-isotropic scattering distribution parameters of the scattering channel and also the antenna placement information to improve the performance of coherent STBC. However, the performance of this scheme profoundly relies on the accuracy of CSI received from the receiver.

4.1 Optimum spatial precoder: coherent STBC

Since $\log(\cdot)$ is a monotonically increasing function, the logarithm of the PEP upper-bound (8) can be used as the objective function (or the cost function). The optimum linear precoder $\mathbf{F}_\mathrm{c}$ is found by solving the optimization problem

$$\begin{aligned}&\min -\log\det\left(\mathbf{I}_{n_\mathrm{T}n_\mathrm{R}} + \frac{\overline{\gamma}\beta_{i,j}}{4}\mathbf{R}_\mathrm{H}\left[\mathbf{I}_{n_\mathrm{R}} \otimes \left(\mathbf{F}_\mathrm{c}\mathbf{F}_\mathrm{c}^\dagger\right)\right]\right)\\ &\text{subject to} \quad \mathrm{tr}\{\mathbf{F}_\mathrm{c}\mathbf{F}_\mathrm{c}^\dagger\} = n_\mathrm{T}.\end{aligned} \tag{9}$$

Since the performance of a communication system is mainly dependent on the PEP of dominant error events, we will design the precoder matrix $\mathbf{F}_\mathrm{c}$ using the value $\beta = \min_{i\neq j}\{\beta_{i,j}\}$. As a result the precoder $\mathbf{F}_\mathrm{c}$ minimizes the error probability of the dominant error event(s). The optimization problem (9) is similar to that considered in [9]. However, [9] derives the optimum precoder in closed form by considering a MISO channel. Below we derive the optimal precoder $\mathbf{F}_\mathrm{c}$ for scheme-2. Note that the optimum precoder $\mathbf{F}_\mathrm{c}$ for scheme-1 can be easily derived from scheme-2 by letting $\mathbf{F}_\mathrm{R} = \mathbf{I}$ and $\mathbf{F}_\mathrm{T} = \mathbf{I}$.

Writing $\mathbf{J}_\mathrm{R}^*\mathbf{F}_\mathrm{R}\mathbf{J}_\mathrm{R}^T$ as the eigen-value decomposition (evd) $\mathbf{J}_\mathrm{R}^*\mathbf{F}_\mathrm{R}\mathbf{J}_\mathrm{R}^T = \mathbf{U}_\mathrm{R}\Lambda_\mathrm{R}\mathbf{U}_\mathrm{R}^\dagger$ and $\mathbf{J}_\mathrm{T}\mathbf{F}_\mathrm{T}\mathbf{J}_\mathrm{T}^\dagger$ as the evd $\mathbf{J}_\mathrm{T}\mathbf{F}_\mathrm{T}\mathbf{J}_\mathrm{T}^\dagger = \mathbf{U}_\mathrm{T}\Lambda_\mathrm{T}\mathbf{U}_\mathrm{T}^\dagger$, and using the Kronecker product identity [17,p. 180] $(\mathbf{A}\otimes\mathbf{C})(\mathbf{B}\otimes\mathbf{D}) = \mathbf{AB}\otimes\mathbf{CD}$, we may write $\mathbf{R}_\mathrm{H}$ as

$$\mathbf{R}_\mathrm{H} = (\mathbf{U}_\mathrm{R}\otimes\mathbf{U}_\mathrm{T})\,(\boldsymbol{\Lambda}_\mathbf{R}\otimes\Lambda_\mathrm{T})\,(\mathbf{U}_\mathrm{R}\otimes\mathbf{U}_\mathrm{T})^\dagger. \tag{10}$$

Substituting (10) in (8), after straight forward manipulations using the matrix determinant identity $\det(\mathbf{I}+\mathbf{AB}) = \det(\mathbf{I}+\mathbf{BA})$ and the Kronecker product identity $(\mathbf{A}\otimes\mathbf{C})(\mathbf{B}\otimes\mathbf{D}) = \mathbf{AB}\otimes\mathbf{CD}$, we can simplify the objective function of optimization problem (9) to

$$-\log\det\left(\mathbf{I}_{n_\mathrm{T}n_\mathrm{R}} + \frac{\overline{\gamma}\beta}{4}\,(\boldsymbol{\Lambda}_\mathbf{R}\otimes\boldsymbol{\Lambda}_\mathbf{T})\,(\mathbf{I}_{n_\mathrm{R}}\otimes\mathbf{U}_\mathrm{T}^\dagger\mathbf{F}_\mathrm{c}\mathbf{F}_\mathrm{c}^\dagger\mathbf{U}_\mathrm{T})\right), \tag{11}$$

where $\beta = \min_{i\neq j}\{\beta_{i,j}\}$ over all possible codewords. Let

$\mathbf{Q}_\mathrm{c} = \frac{\overline{\gamma}\beta}{4}\mathbf{U}_\mathrm{T}^\dagger\mathbf{F}_\mathrm{c}\mathbf{F}_\mathrm{c}^\dagger\mathbf{U}_\mathrm{T}$

then the objective function (11) becomes

$$-\log\det\left(\mathbf{I}_{n_\mathrm{T}n_\mathrm{R}} + (\boldsymbol{\Lambda}_\mathbf{R}\otimes\boldsymbol{\Lambda}_\mathbf{T})\,(\mathbf{I}_{n_\mathrm{R}}\otimes\mathbf{Q}_\mathrm{c})\right) \tag{12}$$

and $\mathbf{Q}_\mathrm{c}$ must satisfy the power constraint $\mathrm{tr}\{\mathbf{Q}_\mathrm{c}\} = n_\mathrm{T}\overline{\gamma}\beta/4$. It should be noted that $\mathbf{Q}_\mathrm{c}$ in (12) is always positive semi-definite as $\mathbf{Q}_\mathrm{c}{=}\mathbf{B}\mathbf{B}^\dagger$, with $\mathbf{B}{=}\sqrt{(\overline{\gamma}\beta)/4}\,\mathbf{U}_\mathrm{T}^\dagger\mathbf{F}_\mathrm{c}$. The optimum $\mathbf{Q}_\mathrm{c}$ is obtained by solving the optimization problem:

$$\begin{aligned}&\min -\log\det\left(\mathbf{I}_{n_\mathrm{T}n_\mathrm{R}} + (\boldsymbol{\Lambda}_\mathbf{R}\otimes\boldsymbol{\Lambda}_\mathbf{T})\,(\mathbf{I}_{n_\mathrm{R}}\otimes\mathbf{Q}_\mathrm{c})\right)\\ &\text{subject to}\quad \mathbf{Q}_\mathrm{c}\succeq 0,\quad \mathrm{tr}\{\mathbf{Q}_\mathrm{c}\} = \frac{n_\mathrm{T}\overline{\gamma}\beta}{4}.\end{aligned} \tag{13}$$

By applying Hadamard's inequality on $\mathbf{I}_{n_\mathrm{T}n_\mathrm{R}} + (\boldsymbol{\Lambda}_\mathbf{R}\otimes\boldsymbol{\Lambda}_\mathbf{T})\,(\mathbf{I}_{n_\mathrm{R}}\otimes\mathbf{Q}_\mathrm{c})$ gives that this determinant is maximized when $(\boldsymbol{\Lambda}_\mathbf{R}\otimes\boldsymbol{\Lambda}_\mathbf{T})(\mathbf{I}_{n_\mathrm{R}}\otimes\mathbf{Q}_\mathrm{c})$ is diagonal [1]. Therefore $\mathbf{Q}_\mathrm{c}$ must be diagonal as $\boldsymbol{\Lambda}_\mathbf{R}$ and $\boldsymbol{\Lambda}_\mathbf{T}$ are both diagonal. Since $(\boldsymbol{\Lambda}_\mathbf{R}\otimes\boldsymbol{\Lambda}_\mathbf{T})(\mathbf{I}_{n_\mathrm{R}}\otimes\mathbf{Q}_\mathrm{c})$ is a positive semi-definite diagonal matrix with non-negative entries on its diagonal, $\mathbf{I}_{n_\mathrm{T}n_\mathrm{R}} + (\boldsymbol{\Lambda}_\mathbf{R}\otimes\boldsymbol{\Lambda}_\mathbf{T})\,(\mathbf{I}_{n_\mathrm{R}}\otimes\mathbf{Q}_\mathrm{c})$ forms a positive definite matrix. As a result, the objective function of our optimization problem is convex [18, p. 73]. Therefore the optimization problem (13) above is a convex minimization problem because the objective function and inequality constraints are convex and equality constraint is affine.

Let $q_i = [\mathbf{Q}_\mathrm{c}]_{i,i}$, $t_i = [\boldsymbol{\Lambda}_\mathbf{T}]_{i,i}$, and $r_j = [\boldsymbol{\Lambda}_\mathbf{R}]_{j,j}$. Optimization problem (13) then reduces to finding $q_i > 0$ such that

$$\begin{aligned}&\min \quad -\textstyle\sum_{j=1}^{n_\mathrm{R}}\sum_{i=1}^{n_\mathrm{T}}\log(1+t_iq_ir_j)\\ &\text{subject to} \qquad \mathbf{q}\succeq 0,\\ &\qquad\qquad \mathbf{1}^T\mathbf{q} = \tfrac{n_\mathrm{T}\overline{\gamma}\beta}{4},\end{aligned} \tag{14}$$

where $\mathbf{q} = [q_1, q_2, \ldots, q_{n_\mathrm{T}}]^T$ and $\mathbf{1}$ denotes the vector of all ones.

Introducing Lagrange multipliers $\lambda_\mathrm{c}\in\mathbb{R}^{n_\mathrm{T}}$ for the inequality constraints $-\mathbf{q}\preceq 0$ and $\upsilon_\mathrm{c}\in\mathbb{R}$ for the equality constraint $\mathbf{1}^T\mathbf{q} = n_\mathrm{T}\overline{\gamma}\beta/4$, we obtain the Karush–Kuhn–Tucker (K.K.T.) conditions

$$\mathbf{q} \succeq 0, \lambda_c \succeq 0, \quad \mathbf{1}^T\mathbf{q} = \frac{n_T\overline{\gamma}\beta}{4},$$
$$\lambda_i q_i = 0, \quad i = 1, 2, \ldots, n_T,$$
$$-\sum_{j=1}^{n_R} \frac{r_j t_i}{1 + r_j t_i q_i} - \lambda_i + \upsilon_c = 0, \quad i = 1, 2, \cdots, n_T. \tag{15}$$

λ_i in (15) can be eliminated since it acts as a slack variable,[5] giving new K.K.T. conditions

$$\mathbf{q} \succeq 0, \qquad \mathbf{1}^T\mathbf{q} = \tfrac{n_T\overline{\gamma}\beta}{4},$$
$$q_i\left(\upsilon_c - \sum_{j=1}^{n_R} \frac{r_j t_i}{1 + r_j t_i q_i}\right) = 0, \quad i = 1, \ldots, n_T, \tag{16}$$
$$\upsilon_c \geq \sum_{j=1}^{n_R} \frac{r_j t_i}{1 + r_j t_i q_i}, \qquad i = 1, \ldots, n_T. \tag{17}$$

For $n_R = 1$, the optimal solution to (14) is given by the classical "water-filling" solution found in information theory [1]. The optimal q_i for this case is given in Sect. 4.2. For $n_R > 1$, the main problem in finding the optimal q_i for given t_i and r_j, $j = 1, 2, \ldots, n_R$ is the case that, there are multiple terms that involve q_i on (16). Therefore we can view our optimization problem (14) as a *generalized water-filling* problem. In fact the optimum q_i for this optimization problem is given by the solution to a polynomial obtained from (16). In Sect. 4.3 and 4.4, we provide closed form expressions for optimum q_i for $n_R = 2$ and 3 receive antennas and a generalized method which gives optimum q_i for $n_R > 3$ is discussed in Sect. 4.5.

As shown above, the optimal $\mathbf{Q}_c$ is diagonal with $\mathbf{Q}_c = \mathrm{diag}\{q_1, q_2, \ldots, q_{n_T}\}$ and optimal spatial precoder $\mathbf{F}_c$ is obtained by forming

$$\mathbf{F}_c = \sqrt{\frac{4}{\beta\overline{\gamma}}}\mathbf{U}_T\mathbf{Q}_c^{1/2}\mathbf{U}_n^{\dagger},$$

where $\mathbf{U}_n$ is any unitary matrix. In this work, we set $\mathbf{U}_n = \mathbf{I}_{n_T}$.

4.2 MISO channel

Consider a MISO channel where we have n_T transmit antennas and a single receive antenna. The optimization problem involved in this case is similar to the water-filling problem in information theory, which has the optimal solution

$$q_i = \begin{cases} \frac{1}{\upsilon_c} - \frac{1}{t_i}, & \upsilon_c < t_i, \\ 0, & \text{otherwise}, \end{cases} \tag{18}$$

where the water-level $1/\upsilon_c$ is chosen to satisfy

$$\sum_{i=1}^{n_T} \max\left(0, \frac{1}{\upsilon_c} - \frac{1}{t_i}\right) = \frac{n_T\overline{\gamma}\beta}{4}.$$

4.3 $n_T \times 2$ MIMO channel

We now consider the case of n_T transmit antennas and $n_R = 2$ receive antennas. As shown in the Appendix B, the optimum q_i for this case is

$$q_i = \begin{cases} A + \sqrt{K}, & \upsilon_c < t_i(r_1 + r_2), \\ 0, & \text{otherwise}, \end{cases} \tag{19}$$

where υ_c is chosen to satisfy

$$\sum_{i=1}^{n_T} \max\left(0, A + \sqrt{K}\right) = \frac{n_T\overline{\gamma}\beta}{4}$$

with

$$A = \frac{2r_1r_2t_i^2 - \upsilon_c t_i(r_1 + r_2)}{2\upsilon_c r_1 r_2 t_i^2} \quad \text{and}$$
$$K = \frac{\upsilon_c^2 t_i^2(r_1 - r_2)^2 + 4r_1^2r_2^2t_i^4}{2\upsilon_c r_1 r_2 t_i^2}. \tag{20}$$

4.4 $n_T \times 3$ MIMO channel

For the case of n_T transmit antennas and $n_R = 3$ receive antennas, the optimum q_i is given by

$$q_i = \begin{cases} -\frac{a_2}{3a_3} + S + T, & \upsilon_c < t_i(r_1 + r_2 + r_3), \\ 0, & \text{otherwise}, \end{cases} \tag{21}$$

where υ_c is chosen to satisfy

$$\sum_{i=1}^{n_T} \max\left(0, -\frac{a_2}{3a_3} + S + T\right) = \frac{n_T\overline{\gamma}\beta}{4}$$

with

$$S+T = \left[R+\sqrt{Q^3 + R^2}\right]^{1/3} + \left[R - \sqrt{Q^3 + R^2}\right]^{1/3},$$
$$Q = \frac{3a_1a_3 - a_2^2}{9a_3^2}, \quad R = \frac{9a_1a_2a_3 - 27a_0a_3^2 - 2a_2^3}{54a_3^3}$$

$a_3 = \upsilon_c r_1 r_2 r_3 t_i^3$, $a_2 = \upsilon_c t_i^2(r_1r_2 + r_1r_3 + r_2r_3) - 3r_1r_2r_3t_i^3$, $a_1 = \upsilon_c t_i(r_1 + r_2 + r_3) - 2t_i^2(r_1r_2 + r_1r_3 + r_2r_3)$, and $a_0 = \upsilon_c - t_i(r_1 + r_2 + r_3)$. A sketch of the proof of (21) is given in the Appendix-C.

[5] If $g(x) \leq \upsilon$ is a constraint inequality, then a variable λ with the property that $g(x) + \lambda = \upsilon$ is called a slack variable [18].

4.5 A Generalized method

We now discuss a method which allows to find optimum solution to (14) for a system with n_T transmit and n_R receive antennas. The complementary slackness condition $\lambda_i q_i = 0$ for $i = 1, 2, \ldots, n_\mathrm{T}$ states that λ_i is zero unless the ith inequality constraint is active at the optimum. Thus, from (16) we have two cases: (i) $q_i = 0$ for $\upsilon_\mathrm{c} > t_i \sum_{j=1}^{n_\mathrm{R}} r_j$, (ii) $\upsilon_\mathrm{c} = \sum_{j=1}^{n_\mathrm{R}} r_j t_i/(1 + r_j t_i q_i)$ for $q_i > 0$ [18, p. 243]. For the later case, the optimum q_i is found by evaluating the roots of n_Rth order polynomial in q_i, where the polynomial is obtained from $\upsilon_\mathrm{c} = \sum_{j=1}^{n_\mathrm{R}} r_j t_i/(1 + r_j t_i q_i)$. Since the objective function of the optimization problem (14) is convex for $\mathbf{q} > 0$, there exist at least one positive root to the n_Rth order polynomial for $\upsilon_\mathrm{c} < t_i \sum_{j=1}^{n_\mathrm{R}} r_j$. In the case of multiple positive roots, the optimum q_i is the one which gives the minimum to the objective function of (14). In both cases, υ_c is chosen to satisfy the power constraint $\mathbf{1}^T\mathbf{q} = n_\mathrm{T}\overline{\gamma}\beta/4$.

4.6 Spatially uncorrelated receive antennas

If n_R receive antennas are placed ideally within the receiver region such that the spatial correlation between antenna elements is zero (i.e., $\mathbf{J}_\mathrm{R}^\dagger\mathbf{J}_\mathrm{R} = \mathbf{I}$), then the cost function in (14) reduces to a single summation and the optimum q_i is given by the water-filling solution (18) obtained for the MISO channel. This is not to say that such a placement is possible even approximately.

5 Problem setup: differential STBC

For the differential STBC, we again use the average PEP upper bound to derive the optimum spatial precoder $\mathbf{F}_\mathrm{d}$. Below shows the derivation of the average PEP upper bound.

Based on (6), the receiver will erroneously select $\mathbf{S}_j$ when $\mathbf{S}_i$ was actually sent as the kth information matrix if

$$\begin{aligned}&\| \mathbf{y}(k) - \mathbf{y}(k-1)\mathcal{S}_j \|^2 \le \| \mathbf{y}(k) - \mathbf{y}(k-1)\mathcal{S}_i \|^2,\\ &\quad \mathbf{y}(k-1)\mathbf{D}_{i,j}\mathbf{y}^\dagger(k-1) \le 2Re\{\mathbf{w}(k)\Delta_{i,j}^\dagger\mathbf{y}^\dagger(k-1)\},\end{aligned} \tag{22}$$

where $\Delta_{i,j} = \mathcal{S}_j - \mathcal{S}_i = \mathbf{I}_{n_\mathrm{R}} \otimes (\mathbf{S}_j - \mathbf{S}_i)$ and $\mathbf{D}_{i,j} = \Delta_{i,j}\Delta_{i,j}^\dagger = \mathbf{I}_{n_\mathrm{R}} \otimes ((\mathbf{S}_i - \mathbf{S}_j)(\mathbf{S}_i - \mathbf{S}_j)^\dagger)$. For given $\mathbf{y}(k-1)$, the term on the left-hand side of (22) is a constant and the term on the right-hand side is a Gaussian random variable. Let $u = 2Re\{\mathbf{w}(k)\Delta_{i,j}^\dagger\mathbf{y}^\dagger(k-1)\}$, then in the Appendix D we have shown that u has the conditional mean

$$\begin{aligned}\bar{m}_{u|\mathbf{y}(k-1)} &= E\{u \mid \mathbf{y}(k-1)\}\\ &= 2\mathrm{Re}\Big\{\bar{m}_{\mathbf{n}(k-1)|\mathbf{y}(k-1)}(\mathbf{I}_{n_\mathrm{T}n_\mathrm{R}} - \mathcal{S}_i\mathcal{S}_j^\dagger)\mathbf{y}^\dagger\\ &\qquad (k-1)\Big\},\end{aligned}$$

where $\bar{m}_{\mathbf{n}(k-1)|\mathbf{y}(k-1)} = \sigma_n^2\mathbf{y}(k-1)(\mathcal{X}_\mathrm{d}^\dagger(k-1)\mathbf{R}_\mathrm{H}\mathcal{X}_\mathrm{d}(k-1) + \sigma_n^2\mathbf{I}_{n_\mathrm{T}n_\mathrm{R}})^{-1}$, and the conditional variance

$$\begin{aligned}\sigma_{u|\mathbf{y}(k-1)}^2 &= E\left\{\| u - \bar{m}_{u|\mathbf{y}(k-1)} \|^2 \mid \mathbf{y}(k-1)\right\}\\ &= 2\mathbf{y}(k-1)\Delta_{i,j}\\ &\quad\times\left(\sigma_n^2\mathbf{I}_{n_\mathrm{T}n_\mathrm{R}} + \mathcal{S}_i^\dagger\Sigma_{\mathbf{n}(k-1)|\mathbf{y}(k-1)}\mathcal{S}_i\right)\Delta_{i,j}^\dagger\mathbf{y}^\dagger\\ &\quad\times(k-1),\end{aligned}$$

where $\Sigma_{\mathbf{n}(k-1)|\mathbf{y}(k-1)} = \sigma_n^2(\mathbf{I}_{n_\mathrm{T}n_\mathrm{R}} - \sigma_n^2(E_s\mathcal{X}_\mathrm{d}^\dagger(k-1)\mathbf{R}_\mathrm{H}\mathcal{X}_\mathrm{d}(k-1) + \sigma_n^2\mathbf{I}_{n_\mathrm{T}n_\mathrm{R}})^{-1})$.

Recall that $\mathbf{R}_\mathrm{H}$ in $\bar{m}_{\mathbf{n}(k-1)|\mathbf{y}(k-1)}$ and $\Sigma_{\mathbf{n}(k-1)|\mathbf{y}(k-1)}$ is the channel correlation matrix, defined by (10) and $\mathcal{X}_\mathrm{d}(k) = \mathbf{I}_{n_\mathrm{R}} \otimes (\mathbf{F}_\mathrm{d}\mathbf{X}(k))$.

Let $d_{i,j}^2 = \mathbf{y}(k-1)\mathbf{D}_{i,j}\mathbf{y}^\dagger(k-1)$. Based on (22), the PEP condition on received signal $\mathbf{y}(k-1)$ is given by

$$\begin{aligned}&\mathrm{P}(\mathbf{S}_i \to \mathbf{S}_j \mid \mathbf{y}(k-1)) = \Pr(U > d_{i,j}^2),\\ &\quad= \int_{d_{i,j}^2}^{\infty}\frac{1}{\sqrt{2\pi}\sigma}\exp\left(-\frac{(u-\bar{m})^2}{2\sigma^2}\right)\mathrm{d}u\\ &\quad= \mathrm{Q}\left(\frac{d_{i,j}^2 - \bar{m}}{\sigma}\right).\end{aligned} \tag{23}$$

In order to obtain unconditional PEP, we need to average (23) with respect to the distribution of $\mathbf{y}(k-1)$. Unlike in the coherent STBC case, finding unconditional PEP from (23) poses a much harder problem due to the non-zero $\bar{m}_{u|\mathbf{y}(k-1)}$ and complicated $\sigma_{u|\mathbf{y}(k-1)}^2$. However, at asymptotically high SNRs (i.e., keeping E_s constant and $\sigma_n^2 \to 0$) the conditional mean and the conditional variance of u reduce to $\bar{m}_{u|\mathbf{y}(k-1)} = 0$ and $\sigma_{u|\mathbf{y}(k-1)}^2 = 4\sigma_n^2 d_{i,j}^2$, respectively. As shown in the Appendix E, the average PEP can be upper bounded by

$$\mathrm{P}(\mathbf{S}_i \to \mathbf{S}_j) \le \frac{1}{2}\frac{1}{\det\left(\mathbf{I} + \frac{1}{8}\left(\overline{\gamma}\,\mathbf{Z}_\mathrm{d,H} + \mathbf{I}_{n_\mathrm{T}n_\mathrm{R}}\right)\mathbf{D}_{i,j}\right)}, \tag{24}$$

where $\overline{\gamma} = E_s/\sigma_n^2$ is the average SNR at each receive antenna and $\mathbf{Z}_\mathrm{d,H} = \mathcal{X}_\mathrm{d}^\dagger(k-1)\mathbf{R}_\mathrm{H}\mathcal{X}_\mathrm{d}(k-1)$. As for the coherent STBC case, we mainly focus on the space–time modulated constellations with the property (4). Furthermore, similar to [16,19] we assume that code length $L = n_{\mathrm{T}}$. Under this assumption, each code word matrix $\mathbf{S}_i$ in $\mathcal{V}$ will satisfy the unitary property $\mathbf{S}_i\mathbf{S}_i^{\dagger} = \mathbf{I}$ and $\mathbf{S}_i^{\dagger}\mathbf{S}_i = \mathbf{I}$ for $i = 1, 2, \ldots, T$. As a result, $\mathbf{X}(k)$ will also satisfy the unitary property $\mathbf{X}(k)\mathbf{X}^{\dagger}(k) = \mathbf{I}$ and $\mathbf{X}^{\dagger}(k)\mathbf{X}(k) = \mathbf{I}$ for $k = 0, 1, 2, \ldots$. Applying (4) on (24) and then using the unitary property of $\mathbf{X}(k-1)$ and the determinant identity $|\mathbf{I} + \mathbf{AB}| = |\mathbf{I} + \mathbf{BA}|$, after straight forward manipulations, we can simplify the PEP upper bound (24) to

$$\mathrm{P}\left(\mathbf{S}_i \rightarrow \mathbf{S}_j\right) \leq \frac{1}{2} \frac{\left(\frac{8+\beta_{i,j}}{8}\right)^{-n_{\mathrm{T}}n_{\mathrm{R}}}}{\det\left(\mathbf{I}_{n_{\mathrm{T}}n_{\mathrm{R}}} + \frac{\beta_{i,j}\overline{\gamma}}{(8+\beta_{i,j})}\mathbf{R}_{\mathrm{H}}(\mathbf{I}_{n_{\mathrm{R}}} \otimes \mathbf{F}_{\mathrm{d}}\mathbf{F}_{\mathrm{d}}^{\dagger})\right)} \tag{25}$$

Similar to the coherent STBC case considered previously, the optimal precoder $\mathbf{F}_{\mathrm{d}}$ for differential STBC is obtained by minimizing the maximum of all PEP upper-bounds subject to the power constraint $\mathrm{tr}\{\mathbf{F}_{\mathrm{d}}\mathbf{F}_{\mathrm{d}}^{\dagger}\} = n_{\mathrm{T}}$. In this case, by considering two scenarios for the channel correlation matrix $\mathbf{R}_{\mathrm{H}}$, we can propose two schemes for optimum $\mathbf{F}_{\mathrm{d}}$.

Scheme 3 ***Fixed scheme (non-coherent)****: find the optimum $\mathbf{F}_{\mathrm{d}}$ that minimizes the average PEP upper bound (25) for differential STBC, subject to the transmit power constraint tr$\{\mathbf{F}_{\mathrm{d}}\mathbf{F}_{\mathrm{d}}^{\dagger}\} = n_{\mathrm{T}}$, for given transmitter and receiver antenna configurations assuming a rich scattering environment.*

Scheme 4 ***Feedback scheme (non-coherent)****: find the optimum $\mathbf{F}_{\mathrm{d}}$ that minimizes the average PEP upper bound (25) for differential STBC, subject to the transmit power constraint tr$\{\mathbf{F}_{\mathrm{d}}\mathbf{F}_{\mathrm{d}}^{\dagger}\} = n_{\mathrm{T}}$, for given transmitter and receiver antenna configurations assuming the receiver estimates the non-isotropic distribution parameters and feeds them back to the transmitter.*

5.1 Optimum spatial precoder: differential STBC

By taking the logarithm of PEP upper-bound (25) we can write the optimization problem for both above schemes as:

$$\begin{aligned} &\min -\log\det\left(\mathbf{I}_{n_{\mathrm{T}}n_{\mathrm{R}}} + \frac{\beta\overline{\gamma}}{(8+\beta)}\mathbf{R}_{\mathrm{H}}\left[\mathbf{I}_{n_{\mathrm{R}}} \otimes \left(\mathbf{F}_{\mathrm{d}}\mathbf{F}_{\mathrm{d}}^{\dagger}\right)\right]\right) \\ &\text{subject to} \quad \mathrm{tr}\{\mathbf{F}_{\mathrm{d}}\mathbf{F}_{\mathrm{d}}^{\dagger}\} = n_{\mathrm{T}}, \end{aligned} \tag{26}$$

where $\beta = \min_{i \neq j}\{\beta_{i,j}\}$ over all possible codewords.[6] Substitute (10) for $\mathbf{R}_{\mathrm{H}}$ in (26) and let

$$\mathbf{P}_{\mathrm{d}} = \frac{\beta\overline{\gamma}}{(8+\beta)}\mathbf{U}_{\mathrm{T}}^{\dagger}\mathbf{F}_{\mathrm{d}}\mathbf{F}_{\mathrm{d}}^{\dagger}\mathbf{U}_{\mathrm{T}}$$

then the optimum $\mathbf{P}_{\mathrm{d}}$ (hence the optimum $\mathbf{F}_{\mathrm{d}}$) is obtained by solving the optimization problem

$$\begin{aligned} &\min -\log\left|\mathbf{I}_{n_{\mathrm{T}}n_{\mathrm{R}}} + (\mathbf{\Lambda}_{\mathbf{R}} \otimes \mathbf{\Lambda}_{\mathbf{T}})(\mathbf{I}_{n_{\mathrm{R}}} \otimes \mathbf{P}_{\mathrm{d}})\right| \\ &\text{subject to} \quad \mathbf{P}_{\mathrm{d}} \succeq 0,\ \mathrm{tr}\{\mathbf{P}_{\mathrm{d}}\} = \frac{\beta\overline{\gamma}n_{\mathrm{T}}}{(8+\beta)}. \end{aligned}$$

The above optimization problem is identical to the optimization problem derived for coherent STBC, except a different scalar for the equality constraint. Therefore, following Sect. 4.1, here we present the final optimization problem and solutions to it without detail derivations.

Following Sect. 4.1, we can show that the optimum $\mathbf{P}_{\mathrm{d}}$ is diagonal and diagonal entries of $\mathbf{P}_{\mathrm{d}}$ are found by solving the optimization problem

$$\begin{aligned} &\min \quad -\sum_{j=1}^{n_{\mathrm{R}}}\sum_{i=1}^{n_{\mathrm{T}}}\log(1 + t_i p_i r_j) \\ &\text{subject to} \quad \mathbf{p} \succeq 0, \\ &\qquad \mathbf{1}^T\mathbf{p} = \frac{\beta\overline{\gamma}n_{\mathrm{T}}}{(8+\beta)}, \end{aligned} \tag{27}$$

where $p_i = [\mathbf{P}_{\mathrm{d}}]_{i,i}$, $t_i = [\mathbf{\Lambda}_{\mathbf{T}}]_{i,i} r_j = [\mathbf{\Lambda}_{\mathbf{R}}]_{j,j}$, and $\mathbf{p} = [p_1, p_2, \ldots, p_{n_{\mathrm{T}}}]^T$. The precoder $\mathbf{F}_{\mathrm{d}}$ is obtained by forming

$$\mathbf{F}_{\mathrm{d}} = \sqrt{\frac{8+\beta}{\beta\overline{\gamma}}}\mathbf{U}_{\mathrm{T}}\mathbf{P}_{\mathrm{d}}^{1/2}\mathbf{U}_n^{\dagger},$$

where $P_{\mathrm{d}} = \mathrm{diag}\{p_1, p_2, \ldots, p_{n_{\mathrm{T}}}\}$ and $\mathbf{U}_n$ is any unitary matrix.

Similar to the coherent STBC case, when $n_{\mathrm{R}} = 1$, the optimum power loading strategy is identical to the "water-filling" in information theory. When $n_{\mathrm{R}} > 1$, a *generalized water-filling* strategy gives the optimum $\mathbf{P}_{\mathrm{d}}$. The Appendix F gives the optimum p_i for (27) for $n_{\mathrm{R}} = 1, 2, 3$ receive antennas. For other cases, the the generalized method discussed in Sect. 4.5 can be directly applied to obtain the optimum p_i.

6 Simulation results: coherent STBC

This section illustrates the performance improvements obtained from coherent STBC when the precoder $\mathbf{F}_{\mathrm{c}}$ derived in Sect. 4.1 is used. In particular, the performance is evaluated for small antenna separations and

[6] Setting $\beta = \min_{i \neq j}\{\beta_{i,j}\}$ will minimize the error probability of the dominant error event(s).

different antenna geometries at the transmitter and the receiver antenna arrays. In our simulations we use the rate-1 space–time modulated constellation constructed in [5] from orthogonal designs for two and four transmit antennas. Also use the rate 3/4 STBC code for $n_T = 3$ transmit antennas given in [5]. When $n_T = 2$, the modulated symbols $c(k)$ are drawn from the normalized QPSK alphabet $\{\pm 1/\sqrt{2} \pm i/\sqrt{2}\}$ and when $n_T = 3$ and 4, $c(k)$ are drawn from the normalized BPSK alphabet $\{\pm 1/\sqrt{2}\}$.

First, we illustrate the water-filling concept for a MISO system with $n_T = 2, 3.$ and 4 transmit antennas for scheme-1. The transmit antennas are placed in uniform circular array (UCA) and uniform linear array (ULA) configurations with 0.2λ minimum separation between two adjacent antenna elements, and we assume a isotropic scattering environment. For each transmit antenna configuration, Table 1 lists the radius of the transmit aperture, number of effective communication modes at the transmit region and the rank of the transmit side spatial correlation matrix $\mathbf{J}_T\mathbf{J}_T^\dagger$. Note that, in all spatial scenarios, we ensure that $\mathbf{J}_T\mathbf{J}_T^\dagger$ is full rank in order that the average PEP upper bound (8) to hold.

Figure 1 shows the water levels for various SNRs. For a given SNR, the optimal power value q_i is the difference between water-level $1/\upsilon_c$ and base level $1/t_i$, whenever the difference is positive; it is zero otherwise. Note that, with this spatial precoder, the diversity order of the system is determined by the number of non-zero q_i's. It is observed that at low SNRs, only one q_i is non-zero for $n_T = 2$ and 3-UCA cases. In these cases, all the available power is assigned to the highest eigen-mode of $\mathbf{J}_T\mathbf{J}_T^\dagger$ (or to the single dominant eigen-channel of $\mathbf{H}$) and the system is operating in eigen-beamforming mode. With other cases, Fig. 1c–e, systems are operating in between eigen-beam forming and full diversity for small SNRs as well as moderate SNRs. In these cases, the spatial precoder assigns more power to the higher eigen-modes of $\mathbf{J}_T\mathbf{J}_T^\dagger$ (or to dominant eigen-channels of $\mathbf{H}$) and less power to the weaker eigen-modes (or to less dominant eigen-channels of $\mathbf{H}$).

Table 1 Transmit antenna configuration details corresponding to water-filling scenarios considered in Fig. 1

Antenna configuration	Tx aperture radius	Number of modes	Rank($\mathbf{J}_T\mathbf{J}_T^\dagger$)
2-Tx	0.1λ	3	2
3-Tx UCA	0.115λ	3	3
3-Tx ULA	0.2λ	5	3
4-Tx UCA	0.142λ	5	4
4-Tx ULA	0.3λ	7	4

6.1 Performance in Non-isotropic scattering environments

We now illustrate the performance improvements obtained using precoding scheme-1 and scheme-2 in non-isotropic scattering environments. Note that precoder $\mathbf{F}_c$ in scheme-1 is derived based on the antenna configuration information and this scheme does not use any CSI feedback from the receiver. The scheme-2 uses both the antenna configuration details and the scattering environment parameters received from the receiver via feed-back to derive the precoder $\mathbf{F}_c$.

For simplicity, here we only consider[7] non-isotropic scattering at the transmitter region and assume the effective communication modes available at the receiver region are uncorrelated, i.e. $\mathbf{F}_R = \mathbf{I}$, for $n_R > 1$. It was shown in [20] that all azimuth power distribution models give very similar correlation values for a given angular spread, especially for small antenna separations. Therefore, without loss of generality, we restrict our investigation only to the uniform-limited azimuth power distribution, which is defined as follows:

***Uniform-limited azimuth power distribution*:** When the energy is departing uniformly to a restricted range of azimuth angles $\pm\triangle$ around a mean angle of departure (AOD) $\phi_0 \in [-\pi, \pi)$, we have the uniform-limited azimuth power distribution [21]

$$\mathcal{P}(\phi) = \frac{1}{2\triangle}, \quad |\phi - \phi_0| \le \triangle,$$

where $\triangle$ represents the non-isotropic parameter of the azimuth power distribution, which is related to the standard deviation of the distribution (angular spread $\sigma_t = \triangle/\sqrt{3}$). For the above APD, the (m, m')th entry of $\mathbf{F}_T$ is given by

$$\{\mathbf{F}_T\}_{m,m'} = \mathrm{sinc}((m - m')\triangle)e^{i(m-m')\phi_0}. \tag{28}$$

Note that, with scheme-2, transmitter only requires the knowledge of σ_t and ϕ_0 in order to build $\mathbf{F}_T$ using

[7] Due to the reciprocity of the channel, results obtained in this section are also valid in the opposite channel scenario (i.e., arbitrary correlation at the receiver and $\mathbf{F}_T = \mathbf{I}$ at the transmitter).

Fig. 1 Water level ($1/\upsilon_c$) for various SNRs for a MISO system. **a** $n_T = 2$, **b** $n_T = 3$ - UCA, **c** $n_T = 4$ - UCA, **d** $n_T = 3$ - ULA, and **e** $n_T = 4$ - ULA for 0.2λ minimum separation between two adjacent transmit antennas

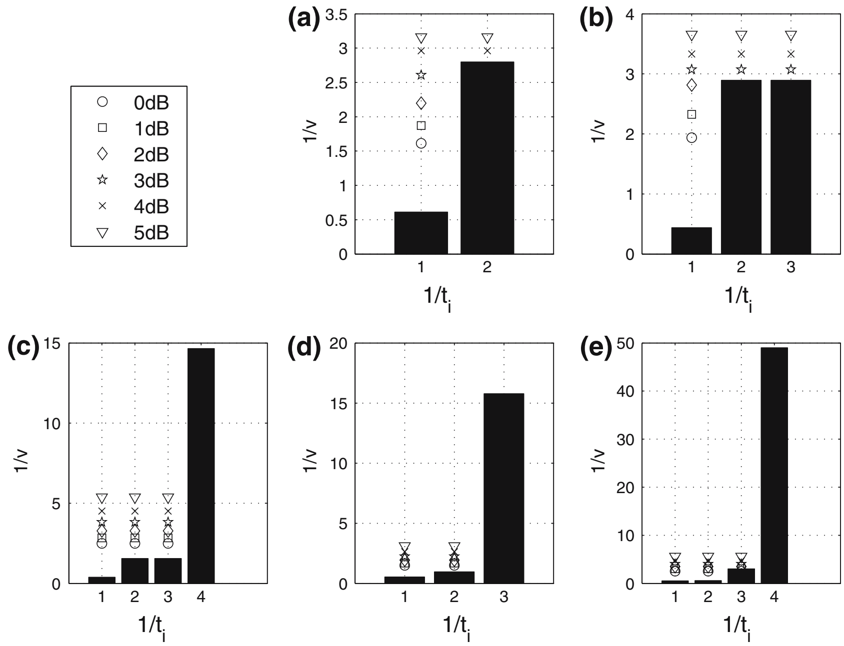

(28), provided that the scattering distribution is unimodal.

In our simulation, a realization of the underlying MIMO channel $\mathbf{H}$ is generated by

$$\mathrm{vec}(\mathbf{H}) = \mathbf{R}_{\mathrm{H}}^{1/2}\mathrm{vec}(\mathbf{H}_{\mathrm{iid}}), \tag{29}$$

where $\mathbf{R}_{\mathrm{H}}^{1/2}$ is the positive definite matrix square root of $\mathbf{R}_{\mathrm{H}}$ and $\mathbf{H}_{\mathrm{iid}}$ is a $n_R \times n_T$ matrix which has zero-mean independent and identically distributed complex Gaussian random entries with unit variance. We use (10) and (29) to generate a realization of the underlying MIMO channel.

Figure 2 illustrates the BER performance of the rate-1 coherent STBC with two-transmit antennas and $n_R = 1, 2$ receive antennas for a uniform-limited azimuth power distribution at the transmitter with angular spread $\sigma_t = 15°$ about the mean AOD $\phi_0 = 0°$. When $n_R = 2$, the two receiver antennas are placed λ apart, giving negligible spatial correlation effects at the receiver due to antenna spacing. From Fig. 2, it is observed that both the fixed scheme (scheme-1) and the feedback scheme (scheme-2) provide significant BER improvements at low SNRs. In fact as discussed earlier, at very low SNRs, the optimum scheme is equivalent to eigen-beam forming.

Further we observe that as the SNR increases, the scheme-1 becomes redundant and the BER performance of scheme-1 approaches that of coherent STBC without precoding and the system is operating in full diversity. This also corroborates the claim that the STBC with two-transmit antennas has good resistance against spatial fading correlation at high SNRs as shown in [22]. In contrast, scheme-2 provides significant BER improvements at high SNRs. However, we expect the performance of scheme-2 to converge to that of coherent STBC without precoding at higher SNRs.

BER performance results of the rate-1 coherent STBC with 4-transmit UCA and 4-transmit ULA antenna configurations[8] are shown in Fig. 3 and 4, respectively, for a uniform-limited azimuth power distribution at the transmitter with angular spread $\sigma_t = 15°$ about the mean AOD $\phi_0 = 0°$. For both antenna configurations, the minimum separation between two adjacent transmit antenna elements is set to 0.2λ. As before, when $n_R = 2$, the two receiver antennas are placed λ apart. For both transmit antenna configurations, simulation results show that the BER performance of both precoding schemes is better than that of the non-precoded system. For example, when $n_R = 2$, it can be seen that at 10^{-3} BER, the performance of scheme-1 is about 2 and 2.5 dB better than that of the non-precoded system for UCA and ULA antenna configurations,

[8] This precoder can be applied to any arbitrary antenna configuration.

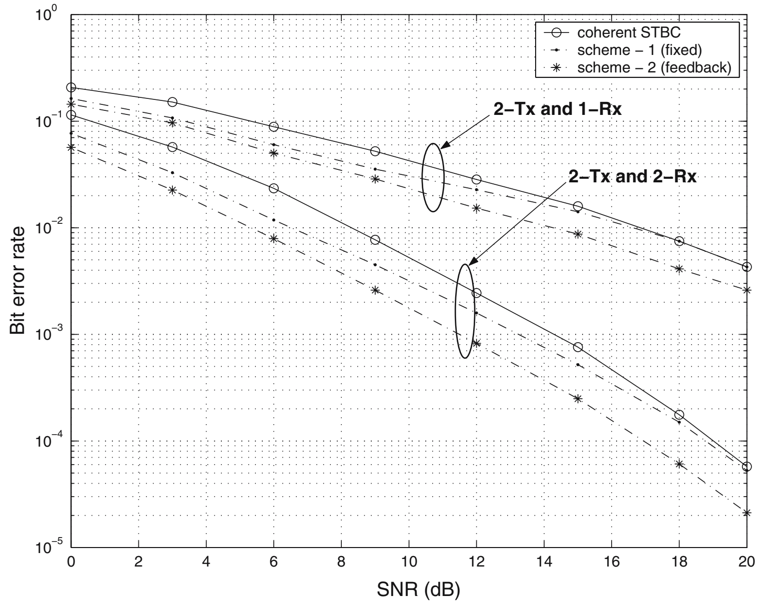

Fig. 2 BER performance of the rate-1 coherent STBC (QPSK) with $n_{\mathrm{T}} = 2$ and $n_{\mathrm{R}} = 1, 2$ antennas; transmit antenna separation 0.2λ

respectively. Also, when $n_{\mathrm{R}} = 2$, we observe that at BER of 10^{-3}, the performance of scheme-2 is about 4 and 6 dB better than that of the non-precoded system for UCA and ULA antenna configurations, respectively. As before, we observe that the performance of scheme-1 converges to the performance of non-precoded system at high SNRs. A similar performance trend is observed with the scheme-2 at higher SNRs. However, with scheme-2, we observe significant BER improvements over all SNRs considered.

At high SNRs, we observed that ULA antenna configuration provides better performance improvements than UCA antenna configuration for both precoding schemes. This is because, the number of effective communication modes in the transmit region is higher for the ULA case (large aperture radius of ULA, cf. Table 1) than the UCA case and both precoding schemes efficiently activate the transmit modes in the transmit region of ULA. This observation suggests that our precoding schemes give scope for improvement of ULA performance at high SNR, especially the fixed scheme.

7 Simulation results: differential STBC

We now demonstrate the performance advantage achieved from precoding schemes proposed in Sect. 5 for differential STBC. In our simulations we use the rate-1 space–time modulated constellations constructed in [5] from orthogonal designs for two and four transmit antennas. Normalized QPSK alphabet $\{\pm 1/\sqrt{2} \pm i/\sqrt{2}\}$ and normalized BPSK alphabet $\{\pm 1/\sqrt{2}\}$ are used with two and four transmit antenna space–time block codes, respectively. As before, a realization of the underlying MIMO channel is simulated using (10) and (29).

Figure 5 illustrates the BER performance of the differential STBC with two-transmit antennas and $n_{\mathrm{R}} = 1, 2$ receive antennas for a uniform-limited azimuth power distribution at the transmitter with angular spread $\sigma_t = 15^\circ$ about the mean AOD $\phi_0 = 0^\circ$. In both cases, two transmit antennas are placed 0.1λ distance apart. When $n_{\mathrm{R}} = 2$, the two receiver antennas are placed λ apart. From Fig. 5, it is observed that both the fixed scheme (scheme-3) and the feedback scheme (scheme-4) provide significant BER improvements at low SNRs. At moderate SNRs (e.g., 8 – 14 dB) we can observe that scheme-3 gives some BER improvement when $n_{\mathrm{R}} = 2$. However as the SNR increases the BER performance of scheme-3 approaches that of differential STBC without precoding. In contrast, scheme-4 provides significant BER improvements at high SNRs and we expect the performance of this scheme to converge to that of differential STBC without precoding at higher SNRs.

Fig. 3 BER performance of the rate-1 coherent STBC (BPSK) with $n_T = 4$ and $n_R = 1, 2$ antennas; UCA transmit antenna configuration

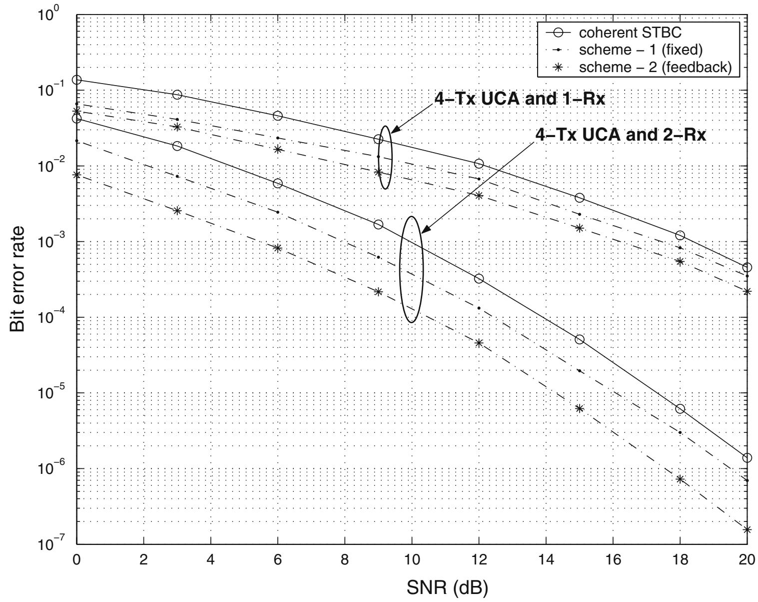

Fig. 4 BER performance of the rate-1 coherent STBC (BPSK) with $n_T = 4$ and $n_R = 1, 2$ antennas; ULA transmit antenna configuration

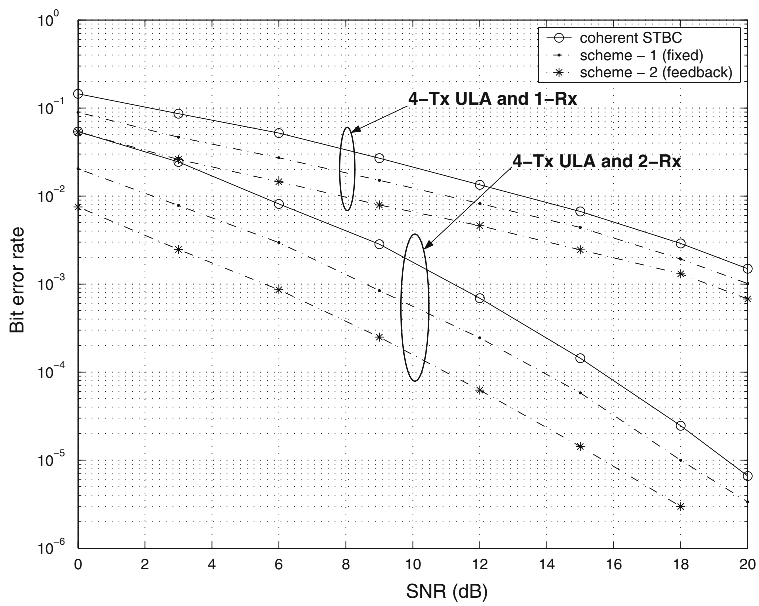

BER performance results for 4-transmit UCA and 4-transmit ULA antenna configurations are shown in Figs. 6 and 7, respectively, for a uniform-limited azimuth power distribution at the transmitter with angular spread $\sigma_t = 15^\circ$ about the mean AOD $\phi_0 = 0^\circ$. For both antenna configurations, the minimum separation between two adjacent transmit antenna elements is set to 0.2λ, corresponding to aperture radii 0.142 and 0.3λ for UCA and ULA antenna configurations, respectively. As before, when $n_R = 2$, the two receiver antennas are placed λ apart. For both transmit antenna configurations, simulation results show that the BER performance of both precoding schemes is better than that of non-precoded systems. For example, when $n_R = 2$, it can be seen that at 10^{-3} BER, the performance of scheme-3 is about 1.5 and 2 dB better than that of the non-precoded system, for UCA and ULA antenna configurations, respectively. As before, we can observe that

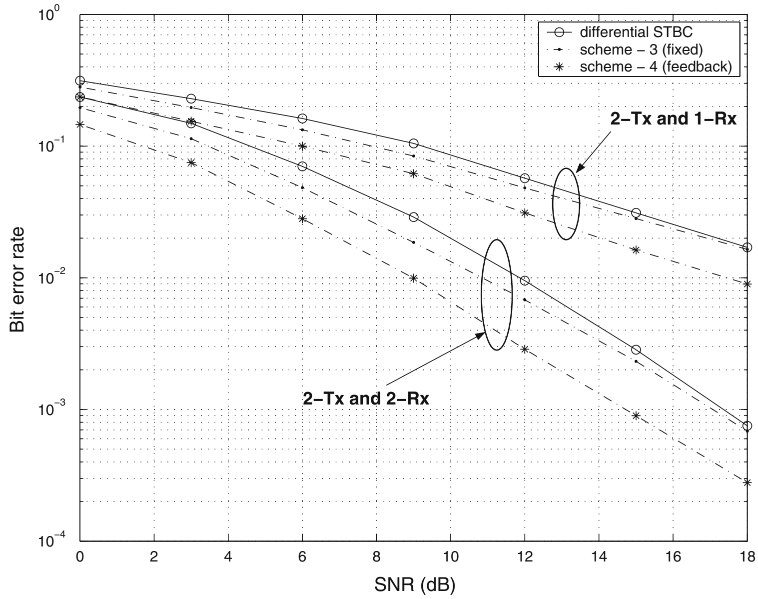

Fig. 5 BER performance of the rate-1 differential STBC (QPSK) with $n_{\mathrm{T}} = 2$ and $n_{\mathrm{R}} = 1, 2$ antennas; transmit antenna separation 0.1λ

the performance of the fixed scheme converges to the performance of the non-precoded system at high SNRs. With the feedback scheme, we observe significant BER improvements over all SNRs considered.

8 Performance in other channel models

Simulation results presented in previous sections used the channel model $\mathbf{H} = \mathbf{J}_{\mathrm{R}}\mathbf{H}_{\mathrm{S}}\mathbf{J}_{\mathrm{T}}^{\dagger}$, which is derived based on plane wave propagation theory, to simulate the underlying channels between transmit and receive antennas. In this section we analyze the performance of fixed precoding scheme (both coherent and differential) derived in this paper applied on other *statistical channel models* proposed in the literature. In particular, we are interested on channel models that are consistent with plane wave propagation theory. MISO and MIMO channel models proposed by Chen et al. [23] and Abdi et al. [24], respectively, are two such example channel models. Sections 8.1 and 8.2 provide simulation results[9] of coherent STBC applied on Chen's MISO channel model and differential STBC applied on Abdi's MIMO channel model, respectively.

[9] Used channel models proposed in [23,24] to model the underlying channel between transmit and receive antennas. Spatial precoders are designed using channel model $\mathbf{H} = \mathbf{J}_{\mathrm{R}}\mathbf{H}_{\mathrm{S}}\mathbf{J}_{\mathrm{T}}^{\dagger}$.

8.1 Chen et al.'s MISO channel model

Figure 8 depicts the MISO channel model proposed by Chen et al., where the space–time cross correlation between two antenna elements at the transmitter is given by

$$[\mathbf{R}(\tau)]_{m,n} = \exp\left[j\frac{2\pi}{\lambda}(d_m - d_n)\right] \times J_0\left[2\pi\sqrt{\left(f_{\mathrm{D}}\tau\cos\gamma + \frac{z_{mn}^c}{\lambda}\right)^2 + \left(f_{\mathrm{D}}\tau\sin\gamma - \frac{z_{mn}^s}{\lambda}\right)^2}\right] \tag{30}$$

with

$$z_{mn}^c = \frac{2a}{d_m + d_n}\left[d_{mn}^{sp} - (d_m - d_n)\cos\alpha_{mn}\cos\beta_{mn}\right],$$
$$z_{mn}^s = \frac{2a}{d_m + d_n}(d_m - d_n)\cos\alpha_{mn}\sin\beta_{mn}$$

a is the scatterer ring radius, γ is the moving direction of the receiver with respect to the end-fire of the antenna array, f_{D} is the Doppler spread and d_{mn} is the receiver distance to the center of the transmit antenna pair m, n. All other geometric parameters are defined as in Fig. 8.

Figure 9 shows the performance of the fixed precoding scheme (scheme-1) derived in Sect. 4.1 for rate-3/4 coherent STBC with three transmit antennas placed in a ULA configuration. In this simulation, we assume the time-varying channels are undergone Rayleigh fading at the fading rate $f_{\mathrm{D}}T = 0.001$, where T is the codeword period. We set parameters $a = 30\lambda$, $d_{12}^{\mathrm{sp}} = d_{23}^{\mathrm{sp}} = 0.2\lambda$, $d_{12} = 1,000\lambda$, $\gamma = 20°$ and $\beta_{1,2} =$

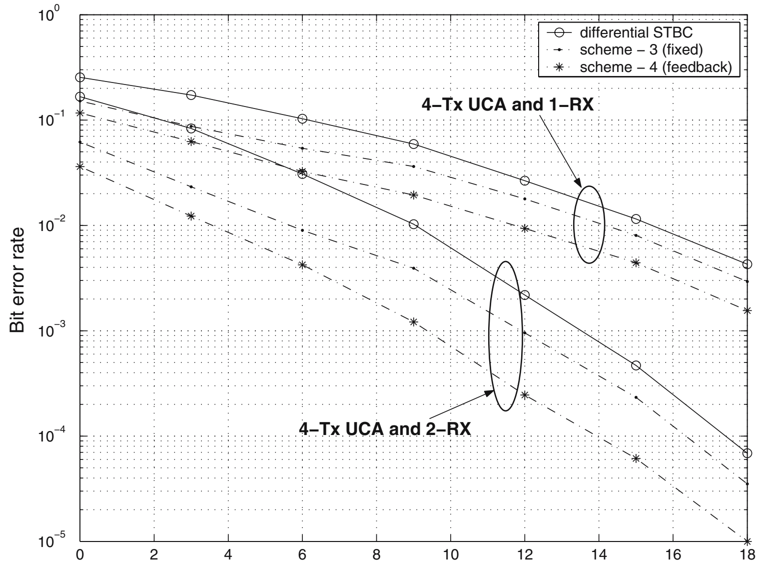

Fig. 6 BER performance of the rate-1 differential STBC (BPSK) with $n_{\mathrm{T}} = 4$ and $n_{\mathrm{R}} = 1, 2$ antennas; UCA transmit antenna configuration

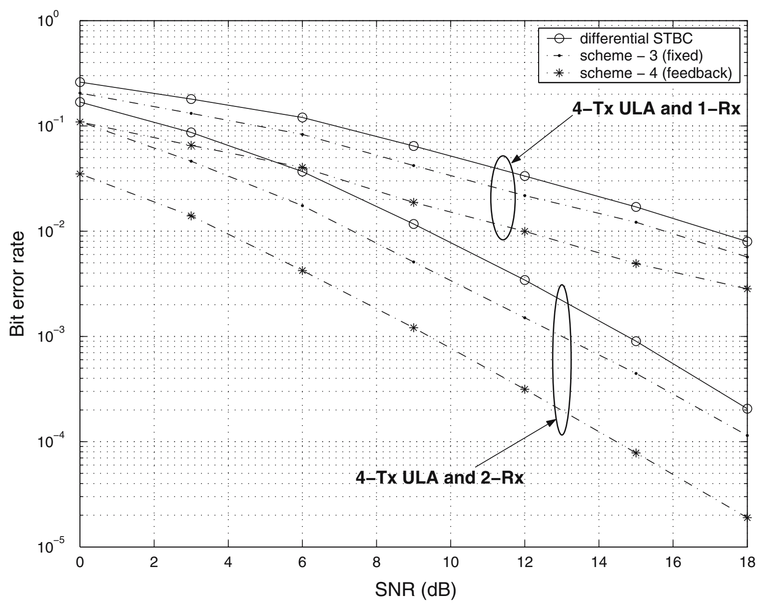

Fig. 7 BER performance of the rate-1 differential STBC (BPSK) with $n_{\mathrm{T}} = 4$ and $n_{\mathrm{R}} = 1, 2$ antennas; ULA transmit antenna configuration

60°. All other geometric parameters of the model in Fig. 8 can be easily determined from these parameters by using simple trigonometry. In this simulation, a realization of the underlying space–time MIMO channel is generated using (29) and (30). From Fig. 9, we observed that proposed fixed precoding scheme gives significant performance improvements for time-varying channels. For example, at 0.05 BER, performance of the spatially precoded system is 1 dB better than that of the non-precoded system.

8.2 Abdi et al.'s MIMO channel model

In this model, space–time cross correlation between two distinct antenna element pairs at the receiver and the transmitter is given by

$$[\mathbf{R}(\tau)]_{lp,mq} = \frac{\exp[jc_{pq}\cos(\alpha_{pq})]}{I_0(\kappa)} \times I_0\Big(\Big\{\kappa^2 - a^2 - b_{lm}^2 - c_{pq}^2\Delta^2\sin^2(\alpha_{pq}) + 2ab_{lm}\cos(\beta_{lm} - \gamma) + 2c_{pq}\Delta\sin(\alpha_{pq})$$

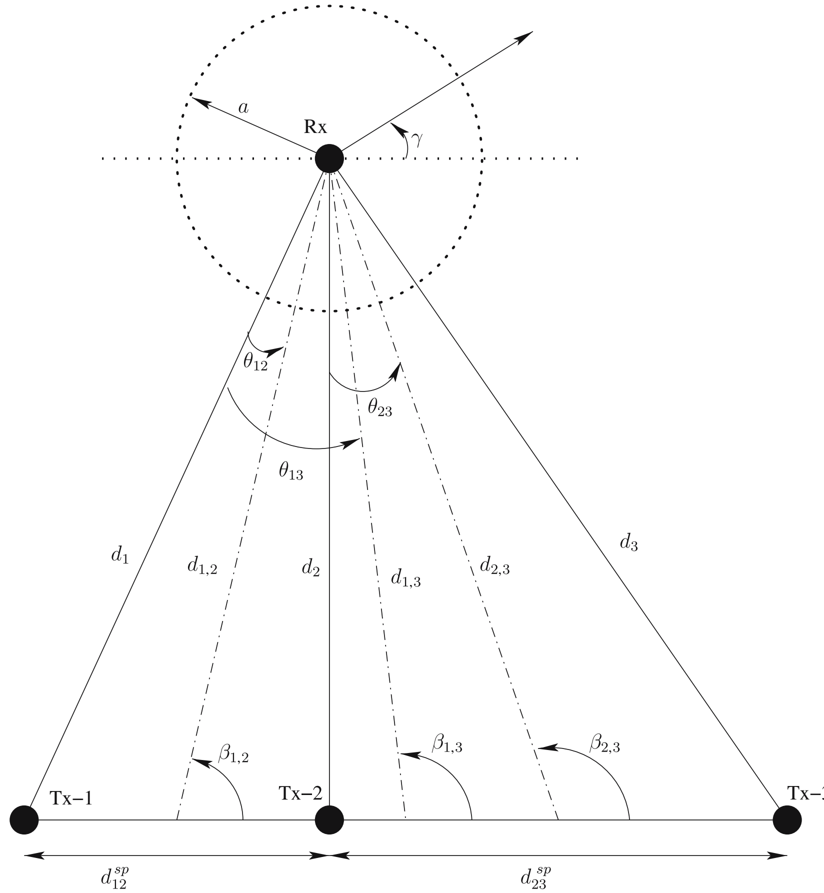

Fig. 8 Scattering channel model proposed by Chen et al. for three transmit and one receive antennas

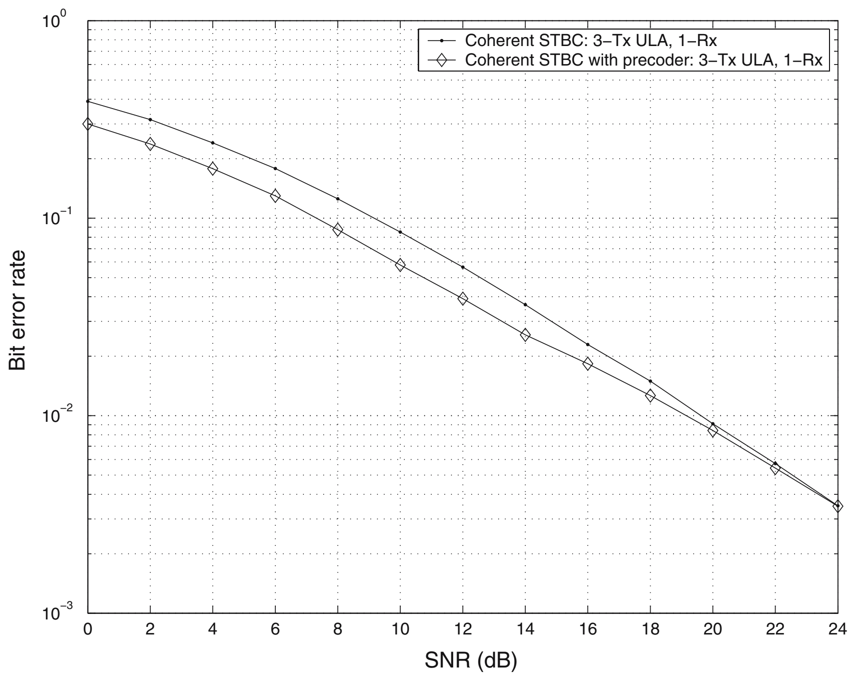

Fig. 9 Spatial precoder performance with three transmit and one receive antennas for 0.2λ minimum separation between two adjacent transmit antennas placed in a uniform linear array, using Chen et al's. channel model: rate-$3/4$ coherent STBC

$$\times\left[a\sin(\gamma)-b_{lm}\sin(\beta_{lm})\right] -j2\kappa\left[a\cos(\varphi_0-\gamma)-b_{lm}\cos(\varphi_0-\beta_{lm}) -c_{pq}\Delta\sin(\alpha_{pq})\sin(\varphi_0)\quad]\right)\}^{1/2}\Big), \qquad (31)$$

where $a=2\pi f_D\tau$, $b_{lm}=2\pi d_{lm}/\lambda$, $c_{pq}=2\pi\delta_{pq}/\lambda$; f_D is the Doppler shift; φ_0 is the mean angle of arrival at the receiver; κ controls the spread of the AOA; and γ is the direction of motion of the receiver. Other geometric parameters are defined in Fig. 10. Note that this model also captures the non-isotropic scattering at the transmitter via Δ and the model is valid only for small Δ [24].

Figure 11 shows the performance of spatial precoder derived in Sect. 5.1 for rate-1 differential STBC with two transmit and two receive antennas for a stationary receiver (i.e., $f_D = 0$). In this simulation, we set $\delta_{12} = 0.1\lambda$, $d_{12} = \lambda$, and $\alpha_{12} = \beta_{12} = 0°$. We assume the scattering environment surrounding the receiver antenna array is rich, i.e., $\kappa = 0$ and the non-isotropic factor Δ at the transmitter is 10°. A realization of the underlying MIMO channel is generated using (29) and (31). It is observed that our precoding scheme based on antenna configuration details give promising improvements for low SNRs when the underlying channel is modeled using Abdi's channel model.

Therefore, using the previous results from Chen's channel model and the current results, we can come to the conclusion that our fixed spatial precoding scheme can be applied to any general wireless communication system. Furthermore, our precoder designs and simulation results provide an independent confirmation of the validity of the spatial channel decomposition $\mathbf{H} = \mathbf{J}_R\mathbf{H}_S\mathbf{J}_T^\dagger$ proposed in [13].

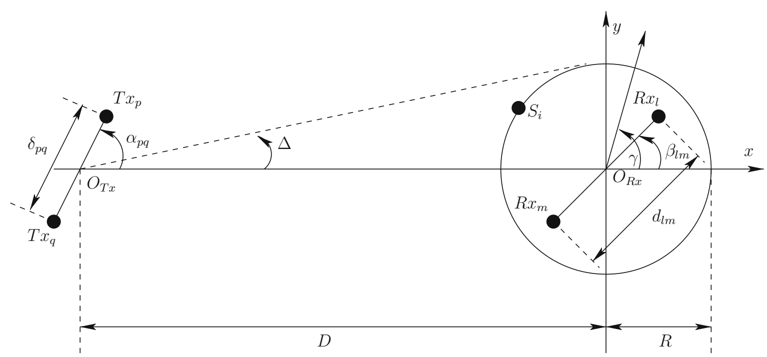

Fig. 10 Scattering channel model proposed by Abdi et al. for two transmit and two receive antennas with local scatters S_i around the mobile receiver

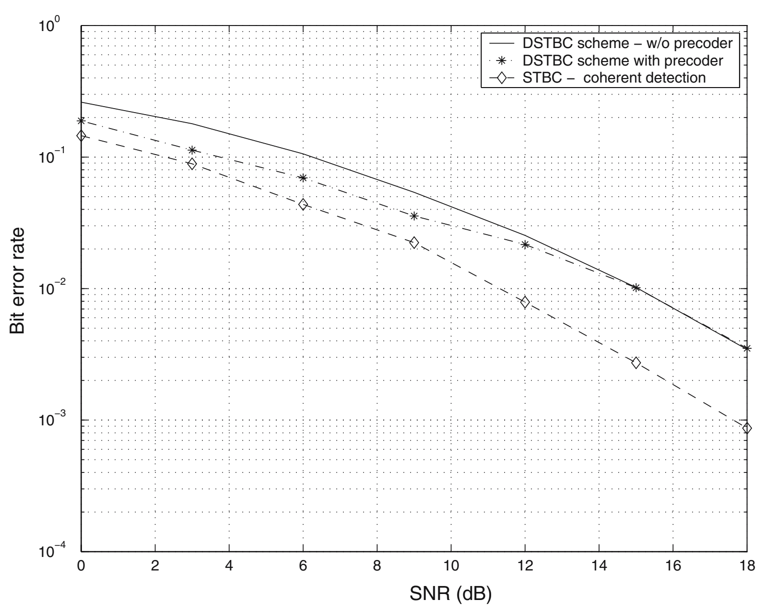

Fig. 11 Spatial precoder performance with two transmit and two receive antennas using Abdi et al.'s channel model: rate-1 differential STBC

9 Concluding remarks

By exploiting the spatial dimension of a MIMO channel, we proposed linear spatial precoding schemes to improve the performance of coherent and non-coherent space–time block coded systems applied on spatially constrained antenna arrays. The proposed precoding schemes are designed based on previously unutilized fixed and known parameters of MIMO channels, the antenna spacing and antenna placement details. Both precoders are fixed for fixed antenna placement and the transmitter does not require any form of feedback of channel state information (partial or full) from the receiver which is an added advantage over the other precoding schemes found in the literature. We also developed linear precoding schemes to exploit the non-isotropic parameters of the scattering channel to improve the performance of space–time codes in non-isotropic scattering environments. Unlike in the fixed scheme, this scheme requires the receiver to estimate the non-isotropic parameters of the scattering channel and feed them back to the transmitter. Based on the simulation results, we observed that the performance of the feedback scheme is superior to that of the fixed scheme for all SNRs in non-isotropic scattering environments. The performance of both precoding schemes is assessed when applied on 1-D antenna arrays (ULA) and 2D antenna arrays (UCA). With 1D antenna arrays, we observed that both fixed and feedback schemes give scope for improvements than with 2D antenna arrays. When $n_\mathrm{T} = 2$, simulation results showed that the fixed scheme provides significant performance improvements at low SNRs and the feedback scheme provides significant performance improvements both at low and high SNRs. However, for $n_\mathrm{T} > 2$, the fixed scheme provides significant performance improvements at moderate SNRs. Based on the performance results, we believe that proposed fixed schemes can be applied on uplink transmission of a mobile communication system as these schemes can effectively reduce the effects due to insufficient antenna spacing and antenna placement at the mobile unit.

Appendix

A Proof of pep upper bound: coherent receiver

The conditional average PEP $\mathrm{P}(\mathbf{S}_i \to \mathbf{S}_j)$, defined as the probability that the receiver erroneously decides in favor of $\mathbf{S}_j$ when $\mathbf{S}_i$ was actually transmitted for a given channel realization, is upper bounded by the *Chernoff bound* [3]

$$\mathrm{P}(\mathbf{S}_i \to \mathbf{S}_j|\mathbf{h}) \le \exp\left(-\frac{\overline{\gamma}}{4} d_h^2(\mathbf{S}_i, \mathbf{S}_j)\right), \tag{32}$$

where $d_h^2(\mathbf{S}_i, \mathbf{S}_j) = \mathbf{h}[\mathbf{I}_{n_\mathrm{R}} \otimes \mathbf{S}_{\Delta,\mathbf{F}_\mathrm{c}}]\mathbf{h}^\dagger$, $\mathbf{S}_{\Delta,\mathbf{F}_\mathrm{c}} = \mathbf{F}_\mathrm{c}(\mathbf{S}_i - \mathbf{S}_j)(\mathbf{S}_i - \mathbf{S}_j)^\dagger \mathbf{F}_\mathrm{c}^\dagger$, $\mathbf{h} = (\mathrm{vec}\{\mathbf{H}^T\})^T$ a row vector and $\overline{\gamma} = E_\mathrm{s}/\sigma_n^2$ is the average SNR at each receive antenna. To compute the average PEP, we average (32) over the joint distribution of $\mathbf{h}$. Assume $\mathbf{h}$ is a proper complex[10] $n_\mathrm{T} n_\mathrm{R}$-dimensional Gaussian random vector with mean $\mathbf{0}$ and covariance matrix $\mathbf{R}_\mathrm{H} = E\left\{\mathbf{h}^\dagger \mathbf{h}\right\}$, then the pdf of $\mathbf{h}$ is given by Goodman [25]

$$p(\mathbf{h}) = \frac{1}{\pi^{n_\mathrm{T} n_\mathrm{R}} \det(\mathbf{R}_\mathrm{H})} \exp\{-\mathbf{h}\mathbf{R}_\mathrm{H}^{-1}\mathbf{h}^\dagger\}$$

provided that $\mathbf{R}_\mathrm{H}$ is non-singular. Then the average PEP is bounded as follows

$$\mathrm{P}(\mathbf{S}_i \to \mathbf{S}_j) \le \frac{1}{\pi^{n_\mathrm{T} n_\mathrm{R}} \det(\mathbf{R}_\mathrm{H})} \int \exp\{-\mathbf{h}\mathbf{R}_0^{-1}\mathbf{h}^\dagger\} \mathrm{d}\mathbf{h} \tag{33}$$

where $\mathbf{R}_0^{-1} = (\frac{\overline{\gamma}}{4}\mathbf{I}_{n_\mathrm{R}} \otimes \mathbf{S}_{\Delta,\mathbf{F}_\mathrm{c}} + \mathbf{R}_\mathrm{H}^{-1})$. Assume $\mathbf{R}_\mathrm{H}$ is non-singular (positive definite), therefore the inverse $\mathbf{R}_\mathrm{H}^{-1}$ is positive definite, since the inverse matrix of a positive definite matrix is also positive definite [17,p. 142]. Also note that $\mathbf{S}_{\Delta,\mathbf{F}_\mathrm{c}}$ is Hermitian and it has positive eigenvalues (through code construction, e.g., [3]), therefore $\mathbf{S}_{\Delta,\mathbf{F}_\mathrm{c}}$ is positive definite, hence $\mathbf{I}_{n_\mathrm{R}} \otimes \mathbf{S}_{\Delta,\mathbf{F}_\mathrm{c}}$ is also positive definite. Therefore $\mathbf{R}_0^{-1}$ is positive definite and hence $\mathbf{R}_0$ is non-singular. Using the normalization property of Gaussian pdf

$$\frac{1}{\pi^{n_\mathrm{T} n_\mathrm{R}} \det(\mathbf{R}_0)} \int \exp\{-\mathbf{h}\mathbf{R}_0^{-1}\mathbf{h}^\dagger\} \mathrm{d}\mathbf{h} = 1$$

we can simplify (33) to

$$\mathrm{P}(\mathbf{S}_i \to \mathbf{S}_j) \le \frac{\det(\mathbf{R}_0)}{\det(\mathbf{R}_\mathrm{H})} = \frac{1}{\det\left(\mathbf{R}_0^{-1}\mathbf{R}_\mathrm{H}\right)}$$

or equivalently

$$\mathrm{P}(\mathbf{S}_i \to \mathbf{S}_j) \le \frac{1}{\det\left(\mathbf{I}_{n_\mathrm{T} n_\mathrm{R}} + \frac{\overline{\gamma}}{4}\mathbf{R}_\mathrm{H}[\mathbf{I}_{n_\mathrm{R}} \otimes \mathbf{S}_{\Delta,\mathbf{F}_\mathrm{c}}]\right)}.$$

B Proof of generalized water-filling solution for $n_\mathbf{R} = 2$ receiver antennas

Let $n_\mathrm{R} = 2$ in (17), then we obtain the second-order polynomial $r_1 r_2 \upsilon_\mathrm{c} t_i^2 q_i^2 + (\upsilon_\mathrm{c} t_i (r_1 + r_2) - 2 r_1 r_2 t_i^2) q_i +$

[10] To be proper complex, the mean of both the real and imaginary parts of $\mathbf{H}_S$ must be zero and also the cross-correlation between real and imaginary parts of $\mathbf{H}_S$ must be zero.

$(\upsilon_c - r_1 t_i - r_2 t_i)$ in q which has roots $q_{i,1} = A + \sqrt{K}$ and $q_{i,2} = A - \sqrt{K}$, where A and K are given by (20). Then the product $q_{i,1}q_{i,2} = (\upsilon_c - r_1 t_i - r_2 t_i)/r_1 r_2 \upsilon_c t_i^2$.

Case 1 *$q_{i,1}q_{i,2} > 0 \Rightarrow \upsilon_c > t_i(r_1 + r_2)$. In this case, both roots are either positive or negative. Let $\upsilon_c = \alpha t_i(r_1+r_2)$, where $\alpha > 1$. Then $A = -t_i^2\alpha[(r_1+r_2)^2 - 2r_1 r_2/\alpha] < 0$ for all $\alpha > 1$. Since $K > 0$, $q_{i,2} < 0$, thus $q_{i,1}$ must also be negative to hold $\upsilon_c > t_i(r_1+r_2)$. Therefore, when $\upsilon_c > t_i(r_1 + r_2)$, the optimum q_i is zero to hold the inequality constraints of (14)*

Case 2 *$q_{i,1}q_{i,2} < 0 \Rightarrow \upsilon_c < t_i(r_1 + r_2)$. In this case, we always have one positive root and one negative root. Assume $q_{i,1} > 0$ and $q_{i,2} < 0$ and let $\upsilon_c = \alpha t_i(r_1+r_2)$, where $0 < \alpha < 1$. For $q_{i,1}$ to positive, we need to prove that $\sqrt{K} > t_i^2\alpha[(r_1 + r_2)^2 - 2r_1 r_2/\alpha]$ for $0 < \alpha < 1$. Instead, we show that*

$$\sqrt{K} < t_i^2\alpha[(r_1 + r_2)^2 - 2r_1 r_2/\alpha], \tag{34}$$

only when $\alpha > 1$. Note that, since $K > 0$, (34) can be squared without affecting to the inequality sign. Therefore squaring (34) and further simplification to it yields $\alpha > 1$. This proves that $q_{i,1} > 0$ and $q_{i,2} < 0$ when $\upsilon_c < t_i(r_1 + r_2)$ and the optimum solution to (14) is given by $q_{i,1}$.

C Proof of generalized water-filling solution for $n_R = 3$ receiver antennas

Let $n_R = 3$ in (17), then we obtain the third-order polynomial $a_3 q_i^3 + a_2 q_i^2 + a_1 q_i + a_0$ in q_i which has roots [26]

$$q_{i,1} = -\tfrac{a_2}{3} + (S + T),$$
$$q_{i,2} = -\tfrac{a_2}{3} - \tfrac{1}{2}(S + T) + \tfrac{\iota\sqrt{3}}{2}(S - T),$$
$$q_{i,3} = -\tfrac{a_2}{3} - \tfrac{1}{2}(S + T) - \tfrac{\iota\sqrt{3}}{2}(S - T),$$

where $S \pm T = \left[R + \sqrt{Q^3+R^2}\right]^{1/3} \pm \left[R - \sqrt{Q^3+R^2}\right]^{1/3}$ and all other variables are as defined in Sect. 4.4, then the product $q_{i,1}q_{i,2}q_{i,3} = (r_1 t_i + r_2 t_i + r_3 t_i - \upsilon_c)/r_1 r_2 r_3 \upsilon_c t_i^3$.

Case 1 *$q_{i,1}q_{i,2}q_{i,3} < 0 \Rightarrow \upsilon_c > t_i(r_1 + r_2 + r_3)$. Let $\upsilon_c = \alpha t_i(r_1 + r_2 + r_3)$, where $\alpha > 1$. For $\alpha > 1$, it can be shown that $(Q^3 + R^2) > 0$, hence $q_{i,1} < 0$ and $q_{i,2}, q_{i,3} \in \mathbb{C}$. Therefore, when $\upsilon_c > t_i(r_1 + r_2 + r_3)$, the optimum q_i is zero.*

Case 2 *$q_{i,1}q_{i,2}q_{i,3} > 0 \Rightarrow \upsilon_c < t_i(r_1 + r_2 + r_3)$. Let $\upsilon_c = \alpha t_i(r_1+r_2+r_3)$, where $0 < \alpha < 1$. For $0 < \alpha < 1$, it can be shown that $(Q^3 + R^2) < 0$ and $R^{1/3} > \frac{a_2}{6}$, hence we get two negative roots $q_{i,2}, q_{i,3} < 0$ and one positive root $q_{i,1} > 0$ as the roots of cubic polynomial. Therefore, when $\upsilon_c < t_i(r_1 + r_2 + r_3)$, the optimum solution to (14) is given by $q_{i,1}$.*

D Proof of the conditional mean and the conditional variance of $u = 2\mathrm{Re}\{\mathbf{w}(k)\Delta_{i,j}^{\dagger}\mathbf{y}^{\dagger}(k-1)\}$

D.1 Proof of conditional mean

Mean of u condition on the received signal $\mathbf{y}(k-1)$ can be written as

$$\begin{aligned}\bar{m}_{u|\mathbf{y}(k-1)} &= E\left\{2Re\left\{\mathbf{w}(k)\Delta_{i,j}^{\dagger}\mathbf{y}^{\dagger}(k-1)\right\} \mid \mathbf{y}(k-1)\right\}\\ &= 2Re\left\{E\left\{\mathbf{w}(k) \mid \mathbf{y}(k-1)\right\}\Delta_{i,j}^{\dagger}\mathbf{y}^{\dagger}(k-1)\right\}.\end{aligned} \tag{35}$$

Substituting $\mathbf{w}(k) = \mathbf{n}(k) - \mathbf{n}(k-1)\mathcal{S}_i$ and noting $E\{\mathbf{n}(k) \mid \mathbf{y}(k-1)\} = 0$, (35) can be simplified to

$$\begin{aligned}\bar{m}_{u|\mathbf{y}(k-1)} &= -2\mathrm{Re}\left\{\bar{m}_{\mathbf{n}(k-1)|\mathbf{y}(k-1)}\mathcal{S}_i\Delta_{i,j}^{\dagger}\mathbf{y}^{\dagger}(k-1)\right\}\\ &= 2\mathrm{Re}\left\{\bar{m}_{\mathbf{n}(k-1)|\mathbf{y}(k-1)}(\mathbf{I}-\mathcal{S}_i\mathcal{S}_j^{\dagger})\mathbf{y}^{\dagger}(k-1)\right\},\end{aligned} \tag{36}$$

where $\bar{m}_{\mathbf{n}(k-1)|\mathbf{y}(k-1)} = E\{\mathbf{n}(k-1) \mid \mathbf{y}(k-1)\}$. Using the minimum mean square error estimator results given in [27,Sect. 2.3], we obtain

$$\begin{aligned}\bar{m}_{\mathbf{n}(k-1)|\mathbf{y}(k-1)} = \; & E\{\mathbf{n}(k-1)\} + \big[\mathbf{y}(k-1)\\ & -E\{\mathbf{y}(k-1)\}\big]\\ & \times\Sigma_{\mathbf{y}(k-1),\mathbf{y}(k-1)}^{-1}\Sigma_{\mathbf{y}(k-1),\mathbf{n}(k-1)},\end{aligned}$$

where

$$\begin{aligned}\Sigma_{\mathbf{y}(k-1),\mathbf{y}(k-1)} &= E\left\{\mathbf{y}^{\dagger}(k-1)\mathbf{y}(k-1)\right\}\\ &= E_s\mathcal{X}_d^{\dagger}(k-1)\mathbf{R}_H\mathcal{X}_d(k-1)\\ &\quad+\sigma_n^2\mathbf{I}_{n_T n_R}\end{aligned} \tag{37}$$

and

$$\begin{aligned}\Sigma_{\mathbf{y}(k-1),\mathbf{n}(k-1)} &= E\left\{\mathbf{y}^{\dagger}(k-1)\mathbf{n}(k-1)\right\}\\ &= \sigma_n^2\mathbf{I}_{n_T n_R}.\end{aligned} \tag{38}$$

Since $E\{\mathbf{n}(k-1)\} = 0$ and $E\{\mathbf{y}(k-1)\} = 0$, we have

$$\begin{aligned}\bar{m}_{\mathbf{n}(k-1)|\mathbf{y}(k-1)} = \; & \sigma_n^2\mathbf{y}(k-1)\\ & \times\left(E_s\mathcal{X}_d^{\dagger}(k-1)\mathbf{R}_H\mathcal{X}_d(k-1) + \sigma_n^2\mathbf{I}\right)^{-1}.\end{aligned} \tag{39}$$

Substituting (39) for $\bar{m}_{\mathbf{n}(k-1)|\mathbf{y}(k-1)}$ in (36) gives the conditional mean $\bar{m}_{u|\mathbf{y}(k-1)}$.

D.2 Proof of conditional variance

Variance of u condition on the received signal $\mathbf{y}(k-1)$ can be written as

$$\begin{aligned}\sigma^2_{u|\mathbf{y}(k-1)} &= E\left\{\|u-\bar{m}_{u|\mathbf{y}(k-1)}\|^2|\ \mathbf{y}(k-1)\right\} \qquad (40)\\ &= E\{(u-\bar{m}_{u|\mathbf{y}(k-1)})^\dagger(u-\bar{m}_{u|\mathbf{y}(k-1)})\\ &\quad \times |\ \mathbf{y}(k-1)\}.\end{aligned}$$

After some straight forward manipulations we can show

$$\begin{aligned}u-\bar{m}_{u|\mathbf{y}(k-1)} = 2\mathrm{Re}\Big\{\Big(&\mathbf{n}(k)-\big[\mathbf{n}(k-1)\\ &-\bar{m}_{\mathbf{n}(k-1)|\mathbf{y}(k-1)}\big]\mathcal{S}_i\Big)\\ &\times \Delta^\dagger_{i,j}\mathbf{y}^\dagger(k-1)\Big\}. \qquad (41)\end{aligned}$$

Now, substituting (41) for $u-\bar{m}_{u|\mathbf{y}(k-1)}$ in (40) gives

$$\begin{aligned}\sigma^2_{u|y(k-1)} = &\ 2\mathbf{y}(k-1)\Delta_{i,j}\\ &\times\left[\Sigma_{\mathbf{n}(k),\mathbf{n}(k)}-\mathcal{S}_i^\dagger\Sigma_{\mathbf{n}(k-1)|\mathbf{y}(k-1)}\mathcal{S}_i\right]\\ &\times\Delta^\dagger_{i,j}\mathbf{y}^\dagger(k-1), \qquad (42)\end{aligned}$$

where $\Sigma_{\mathbf{n}(k),\mathbf{n}(k)} = E\left\{\mathbf{n}^\dagger(k)\mathbf{n}(k)\right\} = \sigma_n^2\mathbf{I}$ and

$$\begin{aligned}\Sigma_{\mathbf{n}(k-1)|\mathbf{y}(k-1)} = &\ E\{\|\mathbf{n}(k-1)-\bar{m}_{n(k-1)|\mathbf{y}(k-1)}\ \|^2\\ &\times |\ \mathbf{y}(k-1)\}\end{aligned}$$

is the covariance of the noise vector $\mathbf{n}(k-1)$ condition on $\mathbf{y}(k-1)$. Using the minimum mean square error estimator results given in [27], we can write

$$\begin{aligned}\Sigma_{\mathbf{n}(k-1)|\mathbf{y}(k-1)} &= \Sigma_{n(k-1),n(k-1)}-\Sigma^\dagger_{\mathbf{y}(k-1),\mathbf{n}(k-1)}\\ &\quad\times\Sigma^{-1}_{\mathbf{y}(k-1),\mathbf{y}(k-1)}\Sigma_{\mathbf{y}(k-1),\mathbf{n}(k-1)}\\ &= \sigma_n^2\left[\mathbf{I}-\sigma_n^2\Sigma^{-1}_{\mathbf{y}(k-1),\mathbf{y}(k-1)}\right]. \qquad (43)\end{aligned}$$

Substituting (37) for $\Sigma_{\mathbf{y}(k-1),\mathbf{y}(k-1)}$ in (43) and then the result in (42) gives the conditional variance $\sigma^2_{u|\mathbf{y}(k-1)}$.

E Proof of pep upper bound: non-coherent receiver

At asymptotically high SNRs, the PEP condition on the received signal $\mathbf{y}(k-1)$ is given by

$$\mathrm{P}(\mathbf{S}_i\to\mathbf{S}_j\mid\mathbf{y}(k-1)) = \mathrm{Q}\left(\sqrt{\frac{d^2_{i,j}}{4\sigma_n^2}}\right).$$

Now using the Chernoff bound

$$\mathrm{Q}(x)\le\frac{1}{2}\exp\left(\frac{-x^2}{2}\right)$$

the conditional PEP can be upper bounded by

$$\mathrm{P}(\mathbf{S}_i\to\mathbf{S}_j\mid\mathbf{y}(k-1))\le\tfrac{1}{2}\exp\left(\frac{-d^2_{i,j}}{8\sigma_n^2}\right). \qquad (44)$$

To compute the average PEP, we average (44) over the joint distribution of $\mathbf{y}(k-1)$. Assume $\mathbf{y}(k-1)$ is a proper complex Gaussian random vector that has mean $E\{\mathbf{y}(k-1)\}=\mathbf{0}$ and covariance

$$\begin{aligned}\mathbf{R}_{\mathbf{y}(k-1)} &\triangleq E\left\{\mathbf{y}^\dagger(k-1)\mathbf{y}(k-1)\right\}\\ &= E_s\mathcal{X}^\dagger_{\mathrm{d}}(k-1)\mathbf{R}_{\mathrm{H}}\mathcal{X}_{\mathrm{d}}(k-1)\\ &\quad+\sigma_n^2\mathbf{I}_{n_{\mathrm{T}}n_{\mathrm{R}}}. \qquad (45)\end{aligned}$$

If $\mathbf{R}_{\mathbf{y}(k-1)}$ is non-singular, then the pdf of $\mathbf{y}(k-1)$ is given by

$$\begin{aligned}p(\mathbf{y}(k-1)) = \frac{\pi^{-n_{\mathrm{T}}n_{\mathrm{R}}}}{\det\left(\mathbf{R}_{\mathbf{y}(k-1)}\right)}\exp\Big\{&-\mathbf{y}(k-1)\mathbf{R}^{-1}_{\mathbf{y}(k-1)}\\ &\mathbf{y}^\dagger\ (k-1)\Big\}.\end{aligned}$$

Averaging (44) over the pdf of $\mathbf{y}(k-1)$, we obtain

$$\begin{aligned}\mathrm{P}(\mathbf{S}_i\to\mathbf{S}_j)\le&\ \frac{\pi^{-n_{\mathrm{T}}n_{\mathrm{R}}}}{2\det\left(\mathbf{R}_{\mathbf{y}(k-1)}\right)}\\ &\times\int\exp\left\{-\mathbf{y}(k-1)\mathbf{R}_{\mathrm{d}}^{-1}\mathbf{y}^\dagger(k-1)\right\}\\ &\mathrm{d}\mathbf{y}(k-1), \qquad (46)\end{aligned}$$

where

$$\mathbf{R}_{\mathrm{d}}^{-1} = \mathbf{R}^{-1}_{\mathbf{y}(k-1)}+\frac{1}{8\sigma_n^2}\mathbf{D}_{i,j}.$$

Assume $\mathbf{R}_{\mathrm{H}}$ is non-singular (positive definite). It can be shown that both $\mathbf{R}_{\mathbf{y}(k-1)}$ and $\mathbf{D}_{i,j}$ are positive definite. Therefore, $\mathbf{R}_{\mathrm{d}}$ is non-singular. Using the normalization property of Gaussian pdf

$$\frac{1}{\pi^{n_{\mathrm{T}}n_{\mathrm{R}}}\det\left(\mathbf{R}_{\mathrm{d}}\right)}\int\exp\left\{-\mathbf{y}(k-1)\mathbf{R}_{\mathrm{d}}^{-1}\mathbf{y}^\dagger(k-1)\right\}\mathrm{d}\mathbf{y}(k-1)=1$$

we can simplify (46) to

$$\mathrm{P}(\mathbf{S}_i\to\mathbf{S}_j)\ \le\frac{\det(\mathbf{R}_{\mathrm{d}})}{2\det(\mathbf{R}_{\mathbf{y}(k-1)})}\ =\frac{1}{2\det\left(\mathbf{R}_{\mathrm{d}}^{-1}\mathbf{R}_{\mathbf{y}(k-1)}\right)}$$

or equivalently

$$\mathrm{P}(\mathbf{S}_i\to\mathbf{S}_j)\le\frac{1}{2}\frac{1}{\det\left(\mathbf{I}+\frac{1}{8}\left(\overline{\gamma}\mathcal{X}^\dagger_{\mathrm{d}}(k-1)\mathbf{R}_{\mathrm{H}}\mathcal{X}_{\mathrm{d}}(k-1)+\mathbf{I}_{n_{\mathrm{T}}n_{\mathrm{R}}}\right)\mathbf{D}_{i,j}\right)}.$$

F optimum precoder for differential STBC

F.1 MISO channel

The optimization problem involved in this case is similar to the water-filling problem in information theory, which has the optimal solution

$$p_i = \begin{cases} \frac{1}{\upsilon_\mathrm{d}} - \frac{1}{t_i}, & \upsilon_d < t_i, \\ 0, & \text{otherwise}, \end{cases} \tag{47}$$

where the water-level $1/\upsilon_d$ is chosen to satisfy

$$\sum_{i=1}^{n_\mathrm{T}} \max\left(0, \frac{1}{\upsilon_\mathrm{d}} - \frac{1}{t_i}\right) = \frac{\overline{\gamma}\beta n_\mathrm{T}}{8+\beta}.$$

F.2 $n_\mathrm{T} \times 2$ MIMO channel

The optimum p_i for this case is

$$p_i = \begin{cases} A + \sqrt{K}, & \upsilon_\mathrm{d} < t_i(r_1 + r_2), \\ 0, & \text{otherwise}, \end{cases}$$

where υ is chosen to satisfy

$$\sum_{i=1}^{n_\mathrm{T}} \max\left(0, A + \sqrt{K}\right) = \frac{\overline{\gamma}\beta n_\mathrm{T}}{8+\beta}$$

with

$$A = \frac{2r_1 r_2 t_i^2 - \upsilon_d t_i (r_1 + r_2)}{2\upsilon_d r_1 r_2 t_i^2}$$

and

$$K = \frac{\upsilon_d^2 t_i^2 (r_1 - r_2)^2 + 4 r_1^2 r_2^2 t_i^4}{2\upsilon_d r_1 r_2 t_i^2}.$$

F.3 $n_\mathrm{T} \times 3$ MIMO channel

For the case of n_T transmit antennas and $n_\mathrm{R} = 3$ receive antennas, the optimum p_i is given by

$$p_i = \begin{cases} -\frac{z_2}{3z_3} + Z, & \upsilon_\mathrm{d} < t_i(r_1 + r_2 + r_3), \\ 0, & \text{otherwise}, \end{cases}$$

where υ_d is chosen to satisfy

$$\sum_{i=1}^{n_\mathrm{T}} \max\left(0, -\frac{z_2}{3z_3} + Z\right) = \frac{\overline{\gamma}\beta n_\mathrm{T}}{8+\beta}$$

with

$$Z = \left[Z_2 + \sqrt{Z_1^3 + Z_2^2}\right]^{1/3} + \left[Z_2 - \sqrt{Z_1^3 + Z_2^2}\right]^{1/3},$$

$$Z_1 = \frac{3z_1 z_3 - z_2^2}{9z_3^2}, \quad Z_2 = \frac{9z_1 z_2 z_3 - 27 z_0 z_3^2 - 2z_2^3}{54 z_3^3}$$

$z_3 = \upsilon_\mathrm{d} r_1 r_2 r_3 t_i^3$, $z_2 = \upsilon_\mathrm{d} t_i^2 (r_1 r_2 + r_1 r_3 + r_2 r_3) - 3 r_1 r_2 r_3 t_i^3$, $z_1 = \upsilon_\mathrm{d} t_i (r_1 + r_2 + r_3) - 2t_i^2 (r_1 r_2 + r_1 r_3 + r_2 r_3)$, and $z_0 = \upsilon_d - t_i (r_1 + r_2 + r_3)$.

Acknowledgements This work was supported by the Australian Research Council Discovery Grant DP0343804. T. D. Abhayapala is also with National ICT Australia, Locked Bag 8001, Canberra, ACT 2601, Australia. National ICT Australia is funded through the Australian Government's *Backing Australia's Ability* initiative, in part through the Australian Research Council.

References

1. Telatar, I. E. (1995). Capacity of multi-antenna gaussian channels. *Tech. Repo., AT & T Bell Labs*.
2. Foschini, G. J., & Gans, M. J. (1998). On limits of wireless communications in a fading environment when using multiple antennas. *Wireless Personal Communications, 6*, 311–335.
3. Tarokh, V., Seshadri, N., & Calderbank, A. R. (1998). Space-time codes for high data rate wireless communication: performance criterion and code construction. *IEEE Transaction Information Theory, 44*(1), 744–765.
4. Alamouti, S. (1998). A simple transmit diversity technique for wireless communications. *IEEE Transaction, Communication, 16*(8), 1451–1458.
5. Tarokh, V., Jafarkhani, H., & Calderbank, A. R. (1999). Space-time codes from orthogonal designs. *IEEE Transaction Information Theory, 45*(5), 1456–1467.
6. Sampath, H., & Paulraj, A. (2001). Linear precoding for space–time coded systems with known fading correlations. In *Proceeding of the asilomar conference signals, systems and computers*, Pacific Grove, CA, USA, Vol. 1, pp. 246–251.
7. Giannakis, G. B., & Zhou S. (2000). Optimal transmit-diversity precoders for random fading channels. In *Proceedings of GLOBECOM*, San Francisco, CA, Vol. 3, pp. 1839–1843.
8. Zhou, S., & Giannakis, G. B. (2003). Optimal transmitter eigen-beamforming and space–time block coding based on channel correlations. *IEEE Transactions Information Theory, 49*, (7), 1673–1690. 2003.
9. Zhao, Y., Adve, R., & Lim, T. J. (2004). Precoding of orthogonal STBC with channel covariance feedback for minimum error probability. In *Proceedings of the 15th IEEE International symposium on personal, indoor and mobile radio communications PIMRC'2004*, Barcelona, Spain.
10. Hjørungnes, A., Akhtae, J., & Gesbert, D. (2004). Precoding for space–time block codes in (non-)kronecker correlated MIMO channels. In *Proceedings of the 12th European signal processing conference, EUSIPCO'2004*, Vienna, Austria, pp. 6–10.
11. Cai, X., & Giannakis, G. B. (2003). Differential space–time modulation with transmit-beamforming for correlated MIMO fading channels. In *Proceedings of the IEEE International Conference on acoustics, speech, and signal processing, 2003 (ICASSP '03)*, Hong Kong Vol. 4, pp. IV–25–28.

12. Nguyen, V. K. (2005). Differential encoding technique for multi-antenna systems with correlated rayleigh fading channels. in *Proceedings of the IEEE International conf. on industrial tech.*, Hong Kong, pp. 1141–1146.
13. Abhayapala, T. D., Pollock, T. S., & Kennedy, R. A. (2003). Spatial decomposition of MIMO wireless channels. In *Proceedings of the 7th international symposium on signal processing and its applications*, Paris, France, Vol. 1, pp. 309–312.
14. Jones, H. M., Kennedy, R. A., & Abhayapala, T. D. (2002). On dimensionality of multipath fields: Spatial extent and richness. In *Proceedings of the IEEE Int. conf. acoust., speech, signal processing, ICASSP'2002*, Orlando, FL, USA Vol. 3, pp. 2837–2840.
15. Lamahewa, T. A., Simon, M. K., Kennedy, R. A., & Abhayapala, T. D. (2005). Performance analysis of space–time codes in realistic propagation environments: A moment generating function-based approach. *Journal Of Communication and Networks, 7*(4), 450–461.
16. Hughes, B. L. (2000). Differential space–time modulation. *IEEE Transaction Information Theory, 46*, 2567–2578.
17. Golub, G. H., & Van Loan, C. F. (1996). *Matrix computations*, (3rd ed.). The Johns Hopkins Baltimore and London: University Press.
18. Boyd, S., & Vandenberghe, L. (2004). *Convex optimization*. Cambridge: Cambridge University Press.
19. Hochwald, B. M., & Sweldens, W. (2000). Differential unitary space–time modulation. *IEEE Transactions on Communication, 48*(12), pp. 2041–2052.
20. Pollock, T. S., Abhayapala, T. D., & Kennedy, R. A. (2003). Introducing space into MIMO capacity calculations. *Journal on Telecommunications Systems (Kluwer Academic Publishers), 24*(2), 415–436.
21. Salz, J., & Winters, J. H. (1994). Effect of fading correlation on adaptive arrays in digital mobile radio. *IEEE Transactions on Vehicular Technology, 42*(4), 1049–1057.
22. Lamahewa, T. A., Abhayapala, T. D., & Kennedy, R. A. (2004). Fading resistance of orthogonal space–time block codes under spatial correlation. In *Proceedings of the IEEE Workshop on signal processing advances in wireless communications, SPAWC*, Lisbon, Portugal, pp. 278–282.
23. Chen, T. A., Fitz, M. P., Kuo, W. Y., Zoltowski, M. D., & Grimm, J. H. (2000). A spacetime model for frequency nonselective rayleigh fading channels with applications to space–time modems. *IEEE Journal on Selected Areas in Communications, 18*, 1175–1190.
24. Abdi, A., & Kaveh, M. (2002). A space–time correlation model for multielement antenna systems in mobile fading channels. *IEEE Journal on Selected Areas in Communications, 20*, 550–560.
25. Goodman, N. R. (1963). Statistical analysis based on a certain multivariate complex gaussian distribution (an introduction). *Annals of Mathematical Statistics, 34*, 152–177.
26. Korn, G. A., & Korn, T. M. (1968). *Mathematical handbook for scientists and engineers*. New York, NY: Dover.
27. Anderson, B. D. O., & Moore, J. B. (2005). *Optimal filtering*. New York: Dover Publications.

Author Biographies

Tharaka A. Lamahewa received the B.Eng. degree in Information Technology and Telecommunications Engineering from the University of Adelaide, South Australia, in 2000. He is currently pursuing the Ph.D. degree in Telecommunications Engineering at the Research School of Information Sciences and Engineering, Australian National University, Canberra. From 2001 to 2003, he worked as a software design engineer at Motorola Electronics Pvt Ltd., Singapore. His research interests include space-time coding, MIMO channel modeling and MIMO capacity analysis for wireless communication systems.

Rodney A. Kennedy received a BE from the University of New South Wales, Australia in 1982, a Master of Engineering from the University of Newcastle in 1986, and a PhD from the Australian National University in 1988. He worked 3 years for CSIRO on the Australia Telescope Project. He is now with the Department of Information Engineering, Research School of Information Sciences and Engineering at the Australian National University. His research interests are in the fields of digital and wireless communications, digital signal processing and acoustical signal processing.

Thushara D. Abhayapala leads the Wireless Signal Processing (WSP) program at the National ICT Australia (NICTA). He is also an Associate Professor at the Australian National University (ANU), Canberra, Australia. He received the B.E.(hons.) degree in interdisciplinary systems engineering in 1994 and the Ph.D. degree in telecommunications Engineering in 1999 from ANU. From 1995 to 1997, he worked as a Research Engineer at the Arthur C. Clarke Centre for Modern Technologies, Sri Lanka. Since December 1999, he has been a faculty member at the Research School of Information Sciences and Engineering, ANU. His research interests are in the areas of space-time signal processing for wireless communication systems, spatiotemporal channel modeling, UWB systems, array signal processing, and acoustic signal processing. He has supervised 20 research students and coauthored over 100 peer reviewed papers. A/Prof. Abhayapala is currently an associate editor for EURASIP Journal on Wireless Communications and Networking.

Van K. Nguyen received his PhD degree in electronic engineering and B.E (honors) degree in computer system engineering from the University of Adelaide in 2004 and 2000, respectively. Since 2003, he has been a Lecturer in the School of Engineering and Technology at Deakin University, Australia. His research interests include multiuser detection for CDMA systems, space-time coding and processing for multiantenna systems, and receiver structure design for general diversity systems.